

1
2
3
4
5
6
7
8
9
10
11
12
13
14
15
16
17
18
19
20
21
22

Mathematical derivation of a refined four-stream radiative transfer model for row planted crops

Xu Ma¹, Tiejun Wang², Lei Lu^{1,3*}

¹ College of Earth and Environmental Sciences, Lanzhou University, Lanzhou, 730000, China,
max15@lzu.edu.cn

² Faculty of Geo-Information Science and Earth Observation (ITC), University of Twente, P.O. Box
217, 7500 AE Enschede, The Netherlands; t.wang@utwente.nl

³ Key Laboratory of Western China's Environmental Systems (Ministry of Education), Lanzhou
University, Lanzhou 730000, China; lulei@lzu.edu.cn

* Correspondence: lulei@lzu.edu.cn; Tel.: +86-151-1721-8663

ABSTRACT:

In the main text, the equations of the results are shown, namely the DRF-related equations. In order to further illustrate our research work, this material provides detailed mathematical physical ideas about the derivation and solution for the modified the four-stream (MFS) radiative transfer equations. The material includes:

- A) Nomenclature table;
- B) Derivation of horizontal radiative transfer equation for row crops;
- C) Area fractions of each component in row crops;
- D) Solving of the DRFs on the boundary of the canopy closure;
- E) Solving of the DRF of between-row based on integral radiative transfer equation.

23 **A. Nomenclature table**

24 Nomenclature table is the symbol of the physical quantities involved in the row
25 modeling of canopy reflectance. Most of the physical quantities follow the original
26 four-stream radiative transfer equations, and only the physical quantities required for
27 the horizontal radiative transfer equations and the row modeling of canopy reflectance
28 are added.

(**Blod:** vector and matrix, **Non-boldface:** scalar)

A-1 Radiance and flux density

Unit: $\text{W m}^{-2} \text{nm}^{-1}$, **General symbol:** E

a) Radiance

Unit: $\text{W m}^{-2} \text{sr}^{-1} \text{nm}^{-1}$, **General symbol:** L

L_i The radiance in the scattering direction

L_o The radiance in the viewing direction

L_b The horizontal radiance of lateral “wall” A

L_d The horizontal radiance of lateral “wall” B

b) Flux density

Unit: $\text{W m}^{-2} \text{nm}^{-1}$, **General symbol:** E

E_s Downward specular irradiance (collimated flux density) on a horizontal plane

E_- Downward Hemispherical diffuse flux density

E_+ Upward Hemispherical diffuse flux density

$E_o(\theta_o)$ Flux-equivalent radiance in the viewing direction

$E_o(\theta_i)$ The Lebesgue integral form of the horizontal radiance (referring to L_b and L_d), and it denotes E_b or E_d with the same radiation energy as $E_o(\theta_o)$

E_b Diffuse horizontal hemispheric flux density through the lateral “wall” A

E_d Diffuse horizontal hemispheric flux density through the lateral “wall” B

A-2 The coefficients and optical functions

Unit: m^{-1}

a) The coefficients of the continuous crops

1-1 The coefficients of the specular flux

k Extinction coefficient for the specular flux

K Extinction coefficient in the viewing direction

s' Forward scatter coefficient for specular flux

S Backscatter coefficient for specular flux

w Bidirectional scattering coefficient

1-2 The coefficients of the uniform diffuse flux

κ Extinction coefficient for diffuse flux, $\kappa = 1$

σ' Forward scattering coefficient for diffuse flux

σ Backscatter coefficient for diffuse flux

a' Absorption coefficient for diffuse flux

a Attenuation coefficient for diffuse flux, $a = a' + \sigma'$

ν Directional backscatter coefficient for diffuse incidence

ν' Directional forward scatter coefficient for diffuse incidence

b) The coefficients of the canopy closure of row crops

1-1 The coefficients of the specular flux

m' Bidirectional scattering coefficient for specular flux to horizontal diffuse flux

o_- Attenuation coefficient of flux from $E_s(0)$ to $E_{||}$

o_+ Enhancement coefficient of flux from $E_s(-1)$ to $E_{||}$

1-2 The coefficients of the uniform diffuse flux

n' Attenuation coefficient for the horizontal diffuse flux

g Radiative converted coefficient describing the proportion of downward diffuse flux converting to horizontal diffuse flux of the lateral “wall”

g' Radiative converted coefficient describing the proportion of upward diffuse flux converting to horizontal diffuse flux of the lateral “wall”

o_1 Attenuation coefficient of flux from $E_-(0)$ to E'_-

o_2 Enhancement coefficient of flux from $E_+(-1)$ to E'_+

o_3 Radiative converted coefficient from E'_\pm to $E_{||}$

1-3 The coefficients of soil particles in the between-row

a_s Attenuation coefficient of soil particle

ω^s Single albedo of soil particle

w^s Bi-directional scattering coefficient of soil particle

b and c Adjustment parameters of soil scattering phase function in the between-row

c) optical function

Unit: dimensionless

G The projection of a unit leaf area onto the surface normal to the direction θ (J.

Ross's G-function)

$p(\delta)$ Scattering phase function of soil particle

K Transfer probability of collision

f_0 Source function of the medium

k Transfer probability (matrix)

A-3 Reflectance, transmittance and radiative transfer ratio

Unit: dimensionless **General symbol:** r (**R**), τ (**T**), ρ (**H**) or g (**G**)

a) Directional reflectance factors on the surface

R_{\perp} Directional reflectance factor (DRF) in the vertical direction

R_{\parallel} DRF in the horizontal direction

R_b DRF of lateral "wall" A

R_d DRF of lateral "wall" B

R_c DRF at the top of canopy closure

R_{br} DRF at the top of between-row

R_{c_1} The single-scattering of the canopy closure

R_{c_m} The multiple-scattering of the canopy closure

R_{br_1} The single-scattering of the between-row

R_{br_m} The multiple-scattering of the between-row

b) Reflectance factors and transmittance factors on the surface

r_{so}^* Bidirectional reflectance on the surface

r_{do}^* Hemispheric-directional reflectance on the surface

r_{sd}^* Directional-hemispherical reflectance on the surface

r_{dd}^* Bi-hemisphere reflectance on the surface

c) Reflectance factor in the layer

r_{so} Bidirectional reflectance in the layer

r_{sd} Directional-hemispherical reflectance in the layer

r_{do} Hemispherical-directional reflectance in the layer

r_{dd} Bi-hemisphere reflectance in the layer

d) Transmittance factor in the layer

τ_{ss} Transmittance in the direction of solar beam in the layer

τ_{sd} Directional-hemispherical transmittance in the layer

τ_{dd} Bi-hemisphere transmittance in the layer

τ_{do} Hemispherical-directional transmittance in the layer

τ_{oo} Transmittance in the direction of observation in the layer

e) Radiative transfer ratio in the layer

$\rho_{d\bar{d}}$ The radiative transfer ratio from downward diffuse to the lateral “wall” in the layer

$\rho'_{d\bar{d}}$ The radiative transfer ratio from upward diffuse to the lateral “wall” in the layer

$\rho_{s\bar{d}}$ The radiative transfer ratio of directional horizontal hemispherical direction in the layer

$\rho_{\bar{d}\bar{d}}$ The radiative transfer ratio of horizontal bi-hemispherical direction in the

layer

f) Single-scattering and multiple-scattering

$r_{so_v}^1$ Single-scattering of specular flux in the canopy closure

$r_{so_v}^m$ Multiple-scattering of specular flux in the canopy closure

$r_{so_s}^1$ Single-scattering of specular flux from the soil in the canopy closure

$r_{so_s}^m$ Multiple-scattering of specular flux between soil and vegetation in the canopy

closure

r_{do}^1 Single-scattering of diffuse flux in the canopy closure

r_{do}^m Multiple-scattering of diffuse flux in the canopy closure

A-4 Angle parameters

Unit: rad, ° **General symbol:** θ (φ)

θ zenith angle

φ Azimuth angle

φ_{so} Relative azimuth angle ($|\varphi_s - \varphi_o|$)

φ_r Row azimuth angle (general symbol of $\varphi_{sr} = |\varphi_s - \varphi_r|$ or $\varphi_{or} = |\varphi_o - \varphi_r|$)

α Inclined angle projected in the perpendicular plane of row canopy

β Azimuth of the inclined angle

Unit: sr **General symbol:** Ω

Ω Solid angle

A-5 Vegetation physical parameters

a) Structural parameter

Unit: m

A_1 Row width

A_2 Distance of between-rows

h The height of the canopy

l The path length of vegetation

N_u Number of row cycle

$f(\theta_i)$ The leaf inclination distribution function (LADF)

$P_o(\Omega, x, z)$ Gap probabilities in the viewing direction

$P_{so}(\Omega_s, \Omega_o, x, z)$ Bi-directional gap probabilities at each point

Ω_E Clumping index

b) Medium-density

Unit: m^{-1}

L' Differential leaf area index (also named as leaf area density) in the vertical direction of the continuous crops

L'_{row} Differential leaf area index for canopy closure in the vertical direction

U Differential leaf area index for the canopy closure in the horizontal direction

Unit: $m m^{-1}$

L Leaf area index

L_{row} Leaf area index for canopy closure

L_E Effective leaf area index

c) Area fraction Unit: dimensionless

$S_{closure_s}(z)$ Fraction of observed canopy illuminated by the specular flux in the canopy closure

$S_{closure_s}(h)$ Fraction of observed soil illuminated by the specular flux in the canopy closure

$S_{closure_d}$ Fraction of canopy closure illuminated by the diffuse flux

$S_{ill_between_row_s}$ Fraction of observed soil background in the between-row area illuminated by the specular flux

$S_{between_row_d}$ Fraction of between-row background illuminated by the diffuse flux

29 **B. Derivation of horizontal radiative** 30 **transfer equation for row crops**

31 Eq. (4) in the main text is $\frac{dE_o(\theta_o)}{L'dz} = wE_s + vE_- + v'E_+ - KE_o(\theta_o)$. It is an
32 approximation of the one-dimensional radiative transfer equation for continuous
33 vegetation [1], and was derived from

$$34 \frac{dE_s}{L'dz} = -kE_s \quad (\text{B-1})$$

$$35 \frac{d\pi L_o}{L'dz} = w(\mu_s, \varphi_s, \mu_o, \varphi_o)E_s + \int_{4\pi} w(\mu_i, \varphi_i, \mu_o, \varphi_o)L_i\mu_i d\Omega_i - K\pi L_o \quad (\text{B-2})$$

36 Similar to Eq. (B-2), the horizontal radiative transfer equation of canopy closure in
37 row planted crops is

$$38 \frac{d\pi L_{||}}{Udx} = m'(\mu_s, \varphi_s, \mu_{i||}, \varphi_{i||})E_s + \int_{4\pi} w(\mu_i, \varphi_i, \mu_{i||}, \varphi_{i||})L_i\mu_i d\Omega_i - n'\pi L_{||} \quad (\text{B-3})$$

39 where the horizontal scattering direction is denoted by $i||$, $L_{||}$ is the horizontal

40 radiance in the lateral “walls” with angles varying between $[-\pi,0)\cup[0,\pi)$ (Fig.
41 B-1(b-c)). m' is the bidirectional scattering coefficient for specular flux to horizontal
42 diffuse flux (its expression reference B-1 in this section), n' is the attenuation
43 coefficient for horizontal diffuse flux. Compared to the attenuation coefficient for
44 vertical diffuse flux (a) [2], n' is computed by using leaf inclined angle rather than
45 normal leaf angle, and $n' = 1 - \frac{\rho + \tau}{2} + \frac{\rho - \tau}{2} \sin^2 \theta_l$, here r and τ are the leaf
46 directional-hemisphere reflectance and transmittance, respectively, θ_l . U is
47 horizontal differential leaf area index, and there is $\int_0^h L'_{row} dz \approx L'_{row} h = \int_{-\frac{A_1}{2}}^{\frac{A_1}{2}} U dx \approx UA_1$,
48 and L'_{row} the differential leaf area index (leaf area density) for canopy closure in the
49 vertical direction, and $L'_{row} = (A_1 + A_2) Lf(\theta_l) d\theta_l / A_1 h$, then there is
50 $U = \frac{(A_1 + A_2) Lf(\theta_l) d\theta_l}{A_1^2}$. Eq. (B-3) is divided into two equations, i.e., the equation

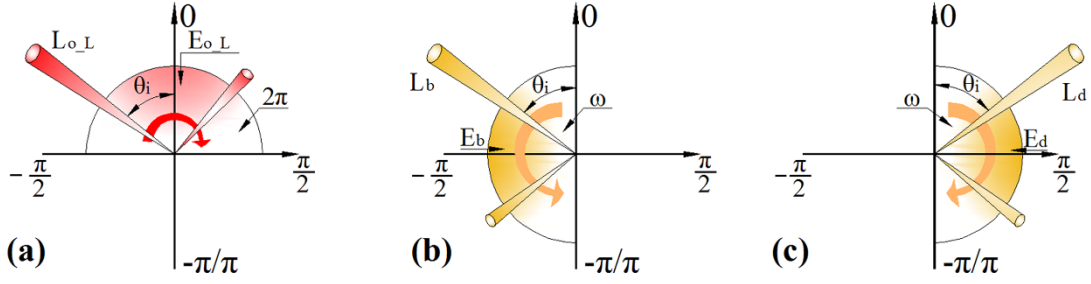
51 describing the horizontal radiative transfer in the lateral “wall” A

$$52 \quad \frac{d\pi L_b}{U dx} = m' E_s + \int_{4\pi} w(\mu_i, \varphi_i, \mu_{i||}, \varphi_{i||}) L_i \mu_i d\Omega_i - n' \pi L_b \quad (\text{B-4})$$

53 and the equation describing the horizontal radiative transfer in the lateral “wall” B

$$54 \quad \frac{d\pi L_d}{U dx} = \int_{4\pi} w(\mu_i, \varphi_i, \mu_{i||}, \varphi_{i||}) L_i \mu_i d\Omega_i - n' \pi L_d \quad (\text{B-5})$$

55 where L_b is the radiance of the lateral “wall” A with angles varying within $[-\pi,0)$
56 (Fig. A-1(b)). L_d is the radiance of the lateral “wall” B with angles varying within
57 $[0,\pi)$ (Fig. B-1(c)).



58

59 Fig. B-1 Sketch of the one-dimensional coordinate system of angle. (a) Zenith angle for the vertical
60 radiation, (b) angle for the radiation of the lateral “wall” A, and (c) angle for the radiation of the
61 lateral “wall” B. The color-coding is explained as: orange+arrow = Riemann integral of the radiance
62 in the horizontal direction, red+arrow = Lebesgue integral of the radiance in the horizontal
63 direction.

64 Eqs. (B, 4-5) are changed into

$$65 \quad \frac{d\pi L_b}{Udx} = m'E_s + \int_{4\pi} w(\mu_i, \varphi_i, \mu_{i\parallel}, \varphi_{i\parallel}) L_i \mu_i d\Omega_i - n' \int_0^\pi L_b d\theta_i \quad (\text{B-6})$$

$$66 \quad \frac{d\pi L_d}{Udx} = \int_{4\pi} w(\mu_i, \varphi_i, \mu_{i\parallel}, \varphi_{i\parallel}) L_i \mu_i d\Omega_i - n' \int_0^\pi L_d d\theta_i \quad (\text{B-7})$$

67 where θ_i is the scattering angle (Fig. A-1(b-c)). $\int_0^\pi L_b d\theta_i$ and $\int_0^\pi L_d d\theta_i$ are the

68 Riemann integral (integral commonly used in calculus, and its illustration see yellow

69 arrow with rotation in Fig. B-1(b-c)). To simplify Eqs. (B, 6-7), $\int_0^\pi L_b d\theta_i$ and $\int_0^\pi L_d d\theta_i$

70 needs to be converted in mathematical form. We give a mathematical **Definition** and

71 **Theorem** in [3].

72 **Definition:** Let $f(x)$ be a bounded function, V is nondegenerate interval, and is

73 recorded as $M_f(V) = \sup\{f(x) | x \in V \cap [a, b]\}$, $m_f(V) = \inf\{f(x) | x \in V \cap [a, b]\}$, $w_f = M(V) - m(V)$.

74 here $w_f(x) = \inf\{w(x) | V \text{ is Open interval, and } x \in V\}$, $w_f(V)$ is the amplitude of f on $x \in$

75 $V \cap [a, b]$, and $w_f(x)$ is the amplitude of f on point x . When the function is determined,

76 $w_f(x)$ and $w_f(V)$ are abbreviated as $w_f(x)$ and $w_f(V)$, respectively.

77 **Theorem:** If the bounded function f is Riemann integrable in $[a,b]$, then a Lebesgue

78 integrable function also exists in $[a,b]$, and their values after integration are equal, i.e.,

79
$$\int_a^b f(x)dx = \int_{[a,b]} f(x)dx .$$

80 According to the **Theorem**, Riemann integrals exist an equal Lebesgue integral

81 (Lebesgue integral is an extension of the Riemann integral on the additive measure of

82 set in real analysis in mathematics, if Riemann integral is understood to divide the

83 integration interval vertically, and Lebesgue integral can divide the value range

84 horizontally. Its illustration see red arrow with rotation in Fig. B-1(a)). Therefore,

85 there are $\int_0^\pi L_b d\theta_i = \int_\omega L_b d\chi$ and $\int_0^\pi L_d d\theta_i = \int_\omega L_d d\chi$, where χ is the Lebesgue measure

86 of the two-dimensional space consisting of the X direction and Z direction, ω is set

87 in additive measure space (i.e., measure space is a mathematical concept), and it

88 varies within $\left[-\frac{\pi}{2}, \frac{\pi}{2}\right] \wedge \left\{ \left[-\frac{\pi}{2}, -\pi\right] \vee \left[\frac{\pi}{2}, \pi\right] \right\}$. Then, Eqs. (B, 6-7) become

89
$$\frac{d\pi L_b}{Udz} = m'E_s + \int_{4\pi} w(\mu_i, \varphi_i, \mu_{i\parallel}, \varphi_{i\parallel}) L_i \mu_i d\Omega_i - n' \int_\omega L_b d\chi \quad (\text{B-8})$$

90
$$\frac{d\pi L_d}{Udz} = \int_{4\pi} w(\mu_i, \varphi_i, \mu_{i\parallel}, \varphi_{i\parallel}) L_i \mu_i d\Omega_i - n' \int_\omega L_d d\chi \quad (\text{B-9})$$

91 The general form of $\int_\omega L_b d\chi$ and $\int_\omega L_d d\chi$ in the Eq. (B, 8-9) is $n'\pi L_{\parallel}$ in Eq. (A-3),

92 and it is obtained by analogy to $K\pi L_o$ in the approximate radiative transfer equation

93 derived by verhoef (i.e., Eq. (B-2)), which represents the extinction of L_o within the

94 layer (i.e., inner canopy closure) (detailed derivation on pages 21-27 in [1]). We

95 assume that the horizontal radiative transfer of horizontal diffuse flux inner (E_b and

96 E_d) canopy closure does not change with height, then vertical radiance in the viewing

97 direction (L_o), radiance of the lateral “wall” A (L_b), and radiance of the lateral “wall”

98 B (L_d) are equal in the canopy closure. Therefore,

$$99 \quad -n' \int_{\omega} L_b d\chi = -n' \int_{\omega} L_o d\chi = -n' \int_0^{\pi} L_o d\theta_i \quad \text{and} \quad -n' \int_{\omega} L_d d\chi = -n' \int_{\omega} L_o d\chi = -n' \int_0^{\pi} L_o d\theta_i. \quad \text{Then,}$$

100 Eqs. (B, 8-9) can be further simplified as

$$101 \quad \frac{d\pi L_b}{Udz} = m'E_s + \int_{4\pi} w(\mu_i, \varphi_i, \mu_{i\parallel}, \varphi_{i\parallel}) L_i \mu_i d\Omega_i - n'E_o(\theta_i) \quad (\text{B-10})$$

$$102 \quad \frac{d\pi L_d}{Udz} = \int_{4\pi} w(\mu_i, \varphi_i, \mu_{i\parallel}, \varphi_{i\parallel}) L_i \mu_i d\Omega_i - n'E_o(\theta_i) \quad (\text{B-11})$$

103 Here $E_o(\theta_i)$ is $E_o(\theta_o)$ in the Eq. (1-d), and just have different mathematical

104 forms, and $E_o(\theta_i)$ is the Lebesgue integral form of the horizontal radiance (L_b and

105 L_d), and it denotes E_b or E_d having the same radiation energy with $E_o(\theta_o)$.

106 According to the analysis of B-1 in the section, then, Eqs. (B, 10-11) are rewritten as

$$107 \quad \frac{dE_b}{Udz} = m'E_s + gE_- + g'E_+ - n'E_o(\theta_i) \quad (\text{B-12})$$

$$108 \quad \frac{dE_d}{Udz} = gE_- + g'E_+ - n'E_o(\theta_i) \quad (\text{B-13})$$

109 In Eqs. (B, 10-11), details of the two issues, including the $\int_{4\pi} w(\mu_i, \varphi_i, \mu_{i\parallel}, \varphi_{i\parallel}) L_i \mu_i d\Omega_i$

110 simplified by the radiative converted coefficient in horizontal diffuse flux, the

111 mathematical form of the bidirectional scattering coefficient for specular flux and

112 horizontal diffuse flux (m'), are clarified as follows.

113 **B-1 Radiative converted coefficient in horizontal diffuse flux**

114 According to Beer’s law and mathematical set theory, the diffuse upward flux

115 through the diagonal area of canopy closure ($E'_+(\ast)$) (When the canopy closure is
 116 assumed in a two-dimensional space, it is a rectangle or square, and the diagonal of
 117 rectangular or square at this time is diagonal area of the canopy closure, i.e., the area
 118 shows in Fig. B-2), the diffuse downward flux through the diagonal area of canopy
 119 closure ($E'_-(\ast)$) and the diffuse internal flux on the surface of the lateral “wall”
 120 ($E_{\parallel}(B)$) are modeled as following formula

$$121 \quad E'_-(\ast) = E_-(0)e^0 - E_-(0)e^{-\kappa L'_{row}\Delta z} - E_-(0)e^{-2\kappa L'_{row}\Delta z} \dots - E_-(0)e^{-3\kappa L'_{row}\Delta z}$$

$$-E_-(0)e^{n\kappa L'_{row}\Delta z} \approx E_-(0) \frac{1}{1+e^{-L'_{row}\Delta z}} = E_-(0)o_1 \quad (\text{B-14})$$

$$122 \quad E'_+(\ast) = E_+(-1)e^0 - E_+(-1)e^{-\kappa L'_{row}\Delta z} - E_+(-1)e^{-2\kappa L'_{row}\Delta z} \dots - E_+(-1)e^{-3\kappa L'_{row}\Delta z}$$

$$-E_+(-1)e^{n\kappa L'_{row}\Delta z} \approx E_+(-1) \frac{1}{1+e^{-L'_{row}\Delta z}} = E_-(0)o_2 \quad (\text{B-15})$$

$$123 \quad E_{\parallel}(B) = n'E'_{\pm}(\ast) = o_3 E'_{\pm}(\ast) \quad (\text{B-16})$$

124 where $E'_{\pm}(\ast)$ denotes $E'_+(\ast)$ and $E'_-(\ast)$. κ is the extinction coefficient for diffuse
 125 flux, and $\kappa = 1$ [2]. The cross-correlation function of the leaves and the normalized
 126 method with 20 sub-layers in the SAIL are used in the step length [1, 4], hence

$$127 \quad \Delta z = -\ln \left[1 - 0.05 \times \left(1 - e^{-\frac{d_{so}}{l'_L}} \right) \right] \frac{l'_L}{d_{so}} \quad (\text{it is an expression derived from the code in the}$$

128 SAIL program), and $d_{so} = \sqrt{\tan^2 \theta_s + \tan^2 \theta_o - 2 \tan \theta_s \tan \theta_o \cos \varphi}$ [1]. Then, the
 129 attenuation coefficient of flux from $E_-(0)$ to E'_- is

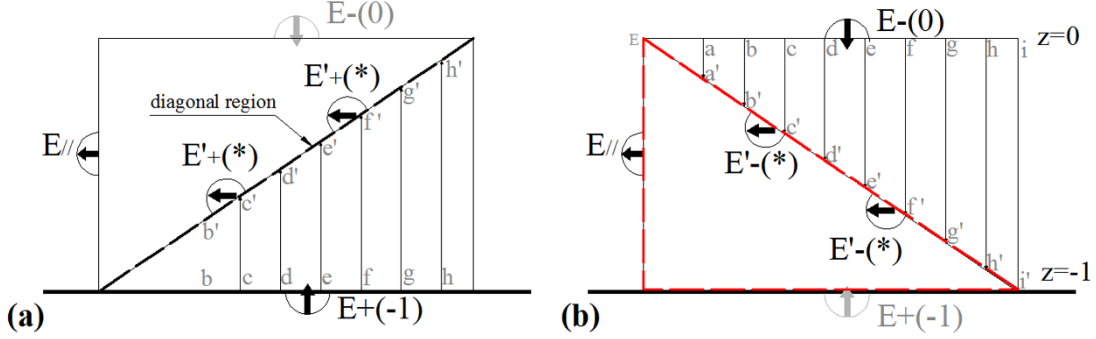
$$130 \quad o_1 = \frac{1}{1+e^{-L'_{row}\Delta z}} \quad (\text{B-17})$$

131 The enhancement coefficient of flux from $E_+(-1)$ to E'_+ is

$$132 \quad o_2 = \frac{1}{1+e^{-L'_{row}\Delta z}} \quad (\text{B-18})$$

133 The radiative converted coefficient from E'_\pm to E_\parallel is

134 $o_3 = n'$ (B-19)



135 (a) Fig. B-2 Sketch of the radiative transfer process of the diffuse flux in the horizontal direction. (a)
 136 Radiative transfer process of diffuse flux from the bottom boundary surface ($E_+(-1)$) to the lateral
 137 “wall” ($E_\parallel(B)$). (b) Radiative transfer process of diffuse flux from the top boundary surface
 138 ($E_-(0)$) to the lateral “wall” ($E_\parallel(B)$). Here, $E'_+(*)$ and $E'_-(*)$ are upward and downward
 139 diffuse flux through the diagonal area, respectively.
 140

141 Combining Eqs. (B, 17-19), the radiative converted coefficient that describes the
 142 proportion of downward diffuse flux converting to horizontal diffuse flux of the
 143 lateral “wall” is

144
$$g = o_3 o_1 = \frac{n'}{1 + e^{-L'_{row} \Delta z}} = \frac{2 - (\sin^2 \theta_l - 1) \rho - (\sin^2 \theta_l + 1) \tau}{2(1 + e^{-L'_{row} \Delta z})}$$
 (B-20)

145 and the radiative converted coefficient that describes the proportion of upward diffuse
 146 flux converting to horizontal diffuse flux of the lateral “wall” is

147
$$g' = o_3 o_2 = \frac{n'}{1 + e^{-L'_{row} \Delta z}} = \frac{2 - (\sin^2 \theta_l - 1) \rho - (\sin^2 \theta_l + 1) \tau}{2(1 + e^{-L'_{row} \Delta z})}$$
 (B-21)

148 **B-2 Bidirectional scattering coefficient for specular flux and**
 149 **horizontal diffuse flux**

150 Coefficients in the four-stream radiative transfer equations are calculated based
 151 on the SAIL model [2]. Thereafter, the coordinate system of the SAIL model is
 152 introduced, and X and Y for row crops are considered. Finally, the coordinate system
 153 of the leaf in row crops is established (Fig. B-3). For one-dimensional radiation
 154 transfer issue, Y is assumed to be an isotropic direction for row crops, hence it is
 155 ignored. Accordingly, the vectors in the generalized coordinates are

156 $\mathbf{l} = (\sin \theta_l \cos \varphi_l; \sin \theta_l \sin \varphi_l; \cos \theta_l)$

157 $\mathbf{s} = (\sin \theta_s; 0; \cos \theta_s)$

158 $\mathbf{o} = (\sin \theta_i \cos \varphi_i; \sin \theta_i \sin \varphi_i; \cos \theta_i)$

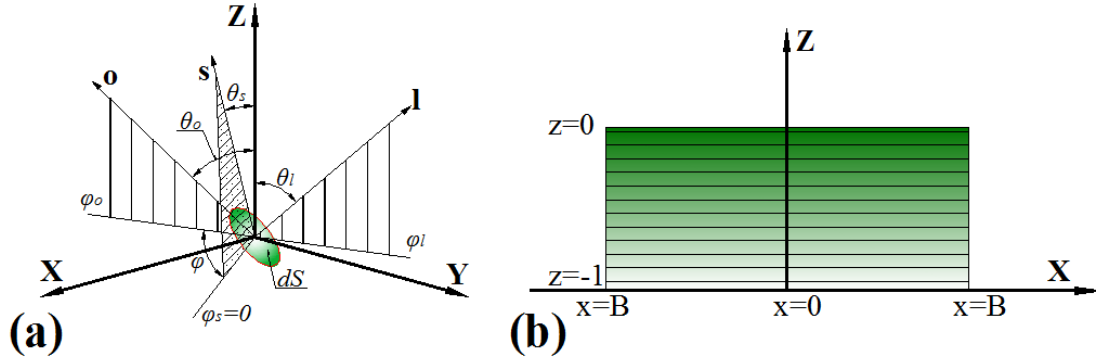
159 $\mathbf{Z} = (0; 0; 1)$

160 $\mathbf{X} = (\pm B; 0; 0)$ (B-22)

161 The horizontal path length of lateral “wall” in the X -axis is $\frac{A_1}{2h} |\sin \varphi_{or}|$, here φ_{or} is
 162 the angle between viewing azimuth (φ_o) angle and row azimuth angle (φ_r). Therefore,
 163 the boundary condition of the canopy closure in the X -axis is

164 $\pm B = \pm \frac{A_1}{2h} |\sin |\varphi_r - \varphi_o||$. Since the direction of the path length is always ignored, the

165 sign of B is removed here, and $B = \frac{A_1}{2h} |\sin |\varphi_r - \varphi_o||$.



166

167 Fig. B-3 Sketch of the orientations of unit vectors \mathbf{l} , \mathbf{s} , \mathbf{o} , \mathbf{X} , \mathbf{Y} , and \mathbf{Z} , relative to the leaf and canopy
 168 closure. (a) The coordinate vector of leaf and (b) the coordinate vector of canopy closure.

169 The vertical conversion factor in the SAIL model is introduced into the
 170 horizontal direction here [2], then the horizontal conversion factor of the solar
 171 direction is

$$172 \quad f_{s\parallel} = (\mathbf{s} \cdot \mathbf{l}) / (\mathbf{s} \cdot \mathbf{X}) = B \cot \theta_s \left[\cos \theta_l (1 + \tan \theta_s \tan \theta_l \cos \varphi_l) \right] = B \cot \theta_s f_s \quad (\text{B-23})$$

173 Here, f_s is the vertical conversion factors in the solar direction [2]. Using the
 174 transition angle in the viewing direction ($\beta_s = \arccos(-1/\tan \theta_o \tan \theta_l)$) [2], $f_{s\parallel}$ can
 175 be divided into two parts

$$176 \quad f_{s\parallel} = f_{s\parallel} + f_{s\perp} = 2 \int_0^{\beta_s} f_{s\parallel} d\varphi_l + 2 \int_0^{\beta_s} -f_{s\parallel} d\varphi_l = 2B \cot \theta_s \cos \theta_l (\beta_s + \tan \theta_s \tan \theta_l \sin \beta_s) \quad (\text{B-24})$$

$$+ 2B \cot \theta_s \cos \theta_l (\beta_s - \pi + \tan \theta_s \tan \theta_l \sin \beta_s) = B \cot \theta_s k$$

177 Eqs. (B, 17-18) are analogized for direct solar radiation, the attenuation coefficient of
 178 flux from $E_s(0)$ to $E_{\parallel_diffuse}$ is

$$179 \quad o_- = \frac{n'}{1 + e^{-kL'_{rov}\Delta z}} \quad (\text{B-25})$$

180 and the enhancement coefficient of flux from $E_s(-1)$ to $E_{\parallel_diffuse}$ is

$$181 \quad o_+ = \frac{n'}{1 + e^{-kL'_{rov}\Delta z}} \quad (\text{B-26})$$

182 Scattering efficiency factors ($Q_{sc}(E_1, E_2)$) similar to the one in SAIL method are

183 used [2], and the bidirectional scattering coefficient for specular flux and horizontal
 184 diffuse flux is

$$\begin{aligned}
 185 \quad m' &= \frac{1}{2\pi} f_{st\parallel}(ro_+ + \tau o_-) + f_{sb\parallel}(ro_+ + \tau o_-) = \frac{1}{2\pi} (f_{st\parallel} + f_{sb\parallel})(ro_+ + \tau o_-) = B \cot \theta_s k (ro_+ + \tau o_-) \\
 &= \frac{A_1 |\sin|\varphi_r - \varphi_o|| \cot \theta_s k (r + \tau) [2 - (\sin^2 \theta_l - 1)\rho - (\sin^2 \theta_l + 1)\tau]}{4h(1 + e^{-kL'_{row}\Delta z})} \quad (B-27)
 \end{aligned}$$

186 Here, r and τ are the leaf directional-hemisphere reflectance and transmittance,
 187 respectively.

188 C. Area fractions of each component in row 189 crops

190 The parameters of S with different subscripts in Eq. (30), Eqs. (32-33), and Eq.
 191 (36-37) in the main text are area fractions of each component (Table C-1), and they
 192 are the integral of the gap probability considering clumping index.

193 Table C-1 Area fractions of each component in the scene

Flux type	Canopy closure	Between-row
Specular flux	$S_{closure_s}(z) = \frac{1}{A_1} \int_0^h \int_0^{A_1} P_{so}(\Omega_s, \Omega_o, x, z) dx dz$	$S_{between_row_s} = \begin{cases} \frac{1}{A_1 + A_2} \int_0^{A_1 + A_2} P_{so}(\Omega_s, \Omega_o, x, h) dx & L < 1 \\ \frac{1}{A_2} \int_{A_1}^{A_1 + A_2} P_{so}(\Omega_s, \Omega_o, x, h) dx & L \geq 1 \end{cases}$
	$S_{closure_s}(h) = \begin{cases} \frac{1}{A_1 + A_2} \int_0^{A_1 + A_2} P_{so}(\Omega_s, \Omega_o, x, h) dx & L < 1 \\ \frac{1}{A_1} \int_0^{A_1} P_{so}(\Omega_s, \Omega_o, x, h) dx & L \geq 1 \end{cases}$	
Diffuse flux	$S_{closure_d} = \frac{1}{A_1} \left[(A_1 + A_2) - \int_{A_2}^{A_1 + A_2} P_o(\Omega_o, x, h) dx - S_{sc} \int_0^{A_1 + A_2} P_o(\Omega_o, x, h) dx \right]$	$S_{between_row_d} = \frac{1}{A_2} \int_{A_1}^{A_1 + A_2} P_o(\Omega_o, x, h) dx$

194 Here $S_{sc} = e^{kL_{row}\Omega E}$

195 Integral in Table C-1 uses the numerical integration method. For the calculation
 196 of the numerical integral, we use Simpson method, which can reduce the cumulative
 197 error to the fourth derivative ($P^{(4)}(v)$ in Table C-2).

198 Table C-2 Numerical integration of Simpson method for Area fractions of each component

Method	Iterative equation	Error of x-axis	Error of z-axis
Simpson method	$\sum_{z=0}^{80} \sum_{x=0}^{40} \frac{d-c}{6} \left\{ 4 \left[\frac{b-a}{6} \left[P(a,c) + 4P\left(\frac{b-a}{2}, z\right) + P(b,c) \right] + \frac{b-a}{6} \left[P\left(a, \frac{d-c}{2}\right) + 4P\left(\frac{b-a}{2}, \frac{d-c}{2}\right) + P\left(b, \frac{d-c}{2}\right) \right] \right] + \left[\frac{b-a}{6} \left[P(a,d) + 4P\left(\frac{b-a}{2}, d\right) + P(b,d) \right] \right] \right\}$	$-\frac{1}{2880}(b-a)^5 P^{(4)}(v), v \in [a, b]$	$-\frac{1}{2880}(d-c)^5 P^{(4)}(v), v \in [d, c]$

199 Here a and b are the starting point and ending point for the integral step in the X-axis, c and d
 200 are the starting point and ending point for the integral step in the Z-axis.

201 For the gap probability in the viewing direction ($P_o(\Omega, x, z)$) and the gap
 202 probability for both sun and viewing directions ($P_{so}(\Omega_s, \Omega_o, x, z)$), [5] gives the
 203 equations without considering the clumping effect of leaves. However, for the leaves
 204 of most crops in the real world, they are not random distribution, but have clumping
 205 effect. According to research in [6, 7], we use clumping index (Ω_E) to modified
 206 equation in [5], and the gap probability considering clumping index in the viewing
 207 direction is

$$208 \quad P_o(\Omega, x, z) = e^{-G(\theta_o) \cdot L'_{row} \cdot l(\Omega_o, x, z) \cdot \Omega_E} \quad (C-1)$$

209 Here $l(\Omega, x, z)$ is the path length of vegetation, and their specific calculation
 210 equation can refer to [8], $G(\theta)$ is the projection of a unit leaf area onto the surface
 211 normal to the direction θ , and it is $k \cos \theta_s$ (or $K \cos \theta_o$, depending on whether it is

212 the solar or the viewing direction). $\Omega_E = \frac{L_E}{L}$, here L_E is the effective leaf area

213 index. The the gap probability considering clumping index for both sun and viewing

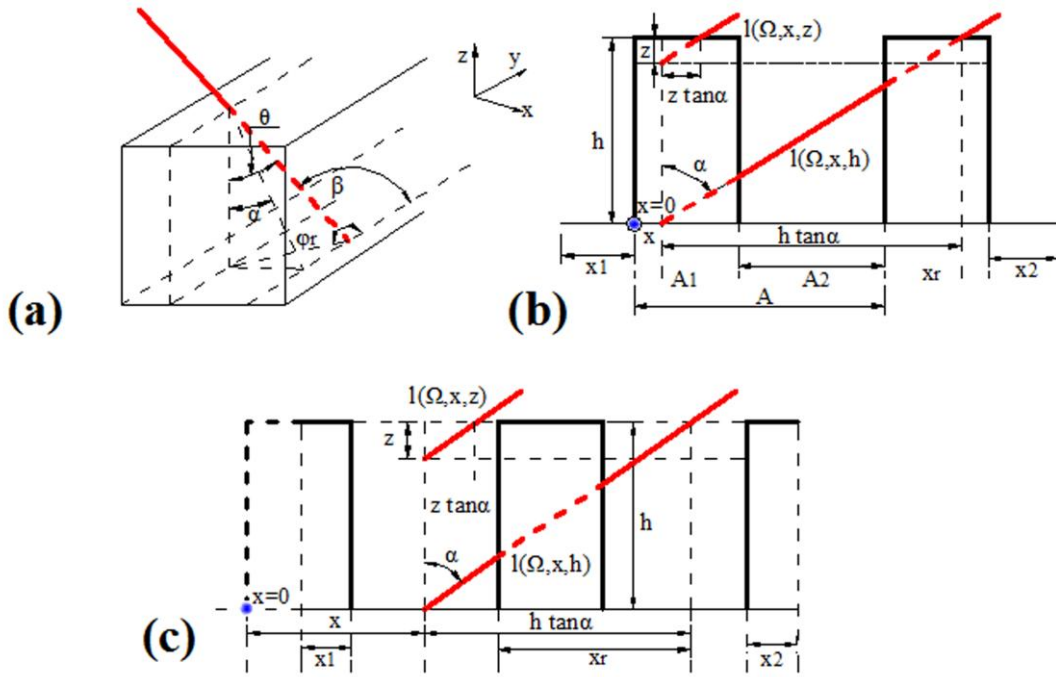
214 directions is

$$\begin{aligned}
 P_{so}(\Omega_s, \Omega_o, x, z) &= P_s(\Omega_s, x, z) P_o(\Omega_o, x, z) C_{hopspot} \\
 &= \exp \left\{ L'_{row} \left[\begin{array}{l} -G(\theta_s) \cdot l_s \cdot \Omega_E - G(\theta_o) \cdot l_o \cdot \Omega_E \\ + \Omega_E \sqrt{G(\theta_s) \cdot l_s \cdot G(\theta_o) \cdot l_o} \frac{l_L^*}{l_{so}} \left(1 - e^{-\frac{l_{so}}{l_L^*}} \right) \end{array} \right] \right\} \quad (C-2)
 \end{aligned}$$

216 here $\cos \xi = \cos \theta_s \cos \theta_o + \sin \theta_s \sin \theta_o \cos |\varphi_s - \varphi_o|$, l_L^* is the canopy dimension
 217 parameter. l_s and l_o are the path length of vegetation in the sun direction and the
 218 path length of vegetation in the viewing direction, respectively.

219 $l_{so} = \sqrt{l_s^2 + l_o^2 - 2l_s l_o \cos \xi}$. In Eqs. (C, 1-2), two key parameters need to be discussed, i.e.,
 220 the path length of vegetation ($l(\Omega, x, z)$) and canopy dimension parameter (l_L^*).

221 C-1 The path length of vegetation



222
 223 Fig. C-1 Sketch of the path length of vegetation and area fractions in row crops. (a) Geometric
 224 relationship of the path length of vegetation; (b) calculation of the path length of vegetation in the
 225 canopy closure; (c) calculation of the path length of vegetation in the between-row. Here, x_1 is the
 226 length of the incomplete area in x-axis at the direction of the incident hemisphere, x_2 is the length of

227 the incomplete area in x-axis at the opposite direction of the incident hemisphere.

228 In the calculation of path length of vegetation, the inclined angle projected in the
229 perpendicular plane of row canopy (α) and the azimuth of inclined angle (β) are
230 defined (Fig. C-1(a)):

$$231 \quad \alpha = \arctan\left(\tan|\theta|\sin\varphi_r\right) \quad (C-3)$$

$$232 \quad \beta = \arcsin\left(\frac{\sin\varphi_r \sin|\theta|}{\sin\alpha}\right) \quad (C-4)$$

233 Where α , β , θ and φ_r are the general symbol, which refers to the solar or the
234 viewing direction, α and β have the sign of positive and negative in the
235 hemisphere space. In the [8], the method to calculate the path length of vegetation in
236 the canopy closure is introduced (Fig. C-1(b)). To calculate the DRFs distribution in
237 row planted crops, the method of calculating path length of vegetation is extended to
238 the between-row background (Fig. C-1(c)) and along row plane (AR). The coordinate
239 origin of X-axes is the vertical bisector of the canopy closure (Fig. B-3(b)), to
240 facilitate the calculation, the coordinate origin of X-axes moved the length of $\frac{A_1}{2}$
241 toward the negative half axis, Therefore, A, A_1, x, x_r have the sign of positive and
242 negative in the hemisphere space. Then, the path length of vegetation is

$$\begin{aligned}
243 \quad l(\Omega, x, z) = & \begin{cases} \frac{N_u A_1 - x - x_r}{\sin \alpha \sin \beta} & (x_r \leq A_1) \wedge (x \leq A_1) \wedge (\theta \neq 0) \wedge [(\varphi_r \neq 0) \vee (\varphi_r \neq 180)] \\ \frac{(N_u + 1) A_1 - x}{\sin \alpha \sin \beta} & (x_r > A_1) \wedge (x \leq A_1) \wedge (\theta \neq 0) \wedge [(\varphi_r \neq 0) \vee (\varphi_r \neq 180)] \\ \frac{[(N_u - 1) A_1 + x_r]}{\sin \alpha \sin \beta} & (x_r \leq A_1) \wedge (x > A_1) \wedge (\theta \neq 0) \wedge [(\varphi_r \neq 0) \vee (\varphi_r \neq 180)] \\ \frac{N_u A_1}{\sin \alpha \sin \beta} & (x_r > A_1) \wedge (x > A_1) \wedge (\theta \neq 0) \wedge [(\varphi_r \neq 0) \vee (\varphi_r \neq 180)] \\ z & (\theta = 0) \wedge (x \leq A_1) \\ 0 & [(\theta = 0) \wedge (x > A_1)] \vee (\varphi_r = 0) \vee (\varphi_r = 180) \\ z / \cos \theta & (\varphi_r = 0) \vee (\varphi_r = 180) \end{cases} \quad (C-5)
\end{aligned}$$

244 Here \wedge and \vee are the mathematical logic symbol for “and” and “or”, respectively.

245 Eq. (C-5) is an example in the positive X-axis. For x on the negative axis, \geq , $>$ and

246 \leq , $<$ need to be interchanged in the limited conditions, while positive sign and

247 negative sign need to be interchanged in the variables. N_u is the number of row

248 cycle, and $N_u = \frac{z \tan \alpha + x - x_r}{A}$. x_r is the remainder of row cycles, and

249 $x_r = \text{mod}\left(\frac{z \tan \alpha + x}{A}\right)$. x and z are X- and Z- axes in the position of space,

250 respectively.

251 C-2 The canopy dimension parameter

252 According to [9], [10] and [5], there are

$$253 \quad l_L^* = \frac{l_L}{h} = \frac{f_L \sqrt{w_* l_*}}{h} \quad (C-6)$$

$$254 \quad l_L^* = \frac{l_L}{h} = \frac{c_L \sqrt{w_* l_*}}{h} \quad (C-7)$$

255 Eqs. (C, 6-7) can apply to the calculation for five-leaf shape (triangle, square,

256 rectangle, ellipse, and circle).

$$257 \quad l_L^* = \frac{l_L}{h} = l^* \sqrt{\frac{w_* \pi}{l_*}} / 2h^2 \quad (C-8)$$

258 Eq. (C-8) is the calculation for the square leaf.

$$259 \quad l_L^* = \frac{l_L}{h} \sqrt{\frac{S_\Delta \pi}{h}} \quad (C-9)$$

260 Eq. (C-9) is the calculation for triangular leaf. Eq. (C-9) come from [5], which cannot
 261 be derived from the literature provided by the paper of DRM (i.e., Eq. (C, 6-8) in this
 262 section). Here l_L^* is the canopy dimension parameter, l_L is an average length of the
 263 chord of leaves. w_* is the average width of the leaf, l_* is the average length of the
 264 leaf. f_L is a correction factor for leaf shape and orientation, c_L is a general
 265 expression for a leaf with an arbitrary shape. S_Δ is the area of triangle leaf.

266 According to [9], the original derivation equation of Eqs. (C, 6-8) is $l_L = \sqrt{A_L}$,
 267 A_L is leaf area. The spatial plane and its chord length do not seem to have the above
 268 mathematical relationship, Eqs. (C, 6-9) are used to calculate the gap probability, and
 269 the physical dimension will have problems. Therefore, the length of an average chord
 270 of leaves is re-derived.

271 a) Elliptic or circular leaves

272 According to the chord length formula of the ellipse in the polar coordinate, the
 273 mean chord length of horizontal leaf for the vertical viewing direction is

$$274 \quad l_{L_hor} = \frac{2ep}{1 - (e \cos \varphi_o)^2} \quad (C-10)$$

275 Where e is eccentricity, and $e = \frac{\sqrt{(0.5 \times l^*)^2 - (0.5 \times w^*)^2}}{(0.5 \times l^*)}$, p is the distance from

276 the ellipse focus to the directrix, and

277
$$p = \frac{(0.5 \times w^*)^2}{\sqrt{(0.5 \times l^*)^2 - (0.5 \times w^*)^2}} + \sqrt{(0.5 \times l^*)^2 - (0.5 \times w^*)^2}$$
. The average chord length of

278 horizontal leaf for the viewing direction will change with the leaf inclination angle

279 from l_{L_hor} to w_* or l_* , respectively. This transformation is a synthesis of affine

280 transformation and orthogonal transformation, and the change coefficient for affine

281 transformation is θ_l (Fig. C-2(b)). Therefore, two equations in two orthogonal

282 directions are derived as

283
$$l_{L_hor1} = \cos \theta_l l_{L_hor} + \sin \theta_l l_*$$
 (C-11)

284
$$l_{L_hor2} = \cos \theta_l l_{L_hor} + \sin \theta_l w_*$$
 (C-12)

285 The plant planting orientation (row azimuth angle for row crops) and spatial

286 distribution of leaves are considered, the average chord length for the alternate or

287 opposite leaves (botanical definition) is

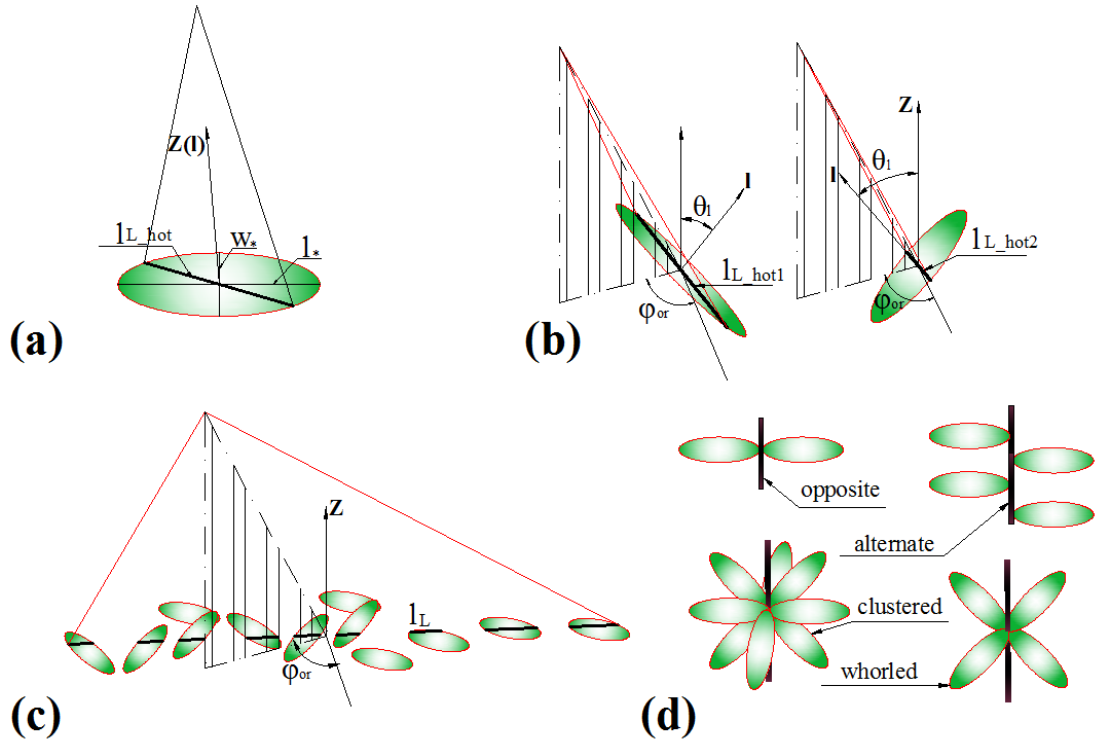
288
$$l_L = |\cos \varphi_{or}| l_{L_hor2} + |\sin \varphi_{or}| l_{L_hor1}$$
 (C-13)

289 This type of distribution includes corn, wheat, etc. The average chord length for the

290 clustered or whorled leaves (botanical definition) is

291
$$l_L = 0.5 \times (l_{L_hor1} + l_{L_hor2})$$
 (C-14)

292 This type of distribution includes beets, potatoes, etc.



293

294 Fig. C-2. The sketch of structure and distribution of ellipse (or circle) leaves. (a) Geometric
 295 relationship of ellipse structure; (b) chord length of leaves under varying leaf inclined angle; (c)
 296 Geometric relationship of average chord length and (d) distribution pattern of leaves on shoots.

297 The canopy dimension parameter is

$$298 \quad l_L^* = \frac{l_L}{h} \quad (C-15)$$

299 Using Eq. (C-15) to calculate gap probability will cause dimensional problems. This
 300 phenomenon is also a problem that is not noticed in the [9], [10] and [5]. According to

301 [1], the relative optical height ($\frac{z}{h}$) is used to modify this problem. Then

$$302 \quad l_L^* = \frac{l_L h}{z} \quad (C-16)$$

303 Using the transformation $\frac{z}{h} \rightarrow z$, and the clumping effect of leaves is considered,

304 therefore, Eq. (C-16) is modified to

305 $l_L^* = \Omega_E l_L h$ (C-17)

306 Combining Eqs. (C, 10-15), the canopy dimension parameter for corn in the paper is

307
$$l_L^* = \begin{cases} \Omega_E h \left\{ \frac{l_*^3 \cos \theta_l (|\sin \varphi_{or}| + |\cos \varphi_{or}|)}{w_*^2 \cos^2 \varphi_o} \right. \\ \left. + \sin \theta_l (|\sin \varphi_{or}| l_* + |\cos \varphi_{or}| w_*) \right\} & (a) \\ \Omega_E h \left\{ \frac{l_*^2 \cos \theta_l}{w_*^2 \cos^2 \varphi_o} + 0.5 \sin \theta_l (l_* + w_*) \right\} & (b) \end{cases} \quad (C-18)$$

308 Here the function (a) in Eq. (C-18) is the alternate or opposite leaves, and function (b)
 309 in Eq. (C-18) is the clustered or whorled leaves. The canopy dimension parameter is a
 310 function of the average width of leaf, the average length of leaf, leaf inclined angle,
 311 plant planting orientation (row azimuth angle for row crops), the height of the canopy,
 312 the spatial distribution of leaves and leaf shape. The average width of the leaf (w_*)
 313 and the average length of the leaf (l_*) in Eq. (C-18) are very easy to measure.

314 **b) Triangular leaves**

315 Considering the comparison of RGM (the mian text), the triangular leaves are
 316 used. The triangle has no chord length, and the side length is used for derivation. $l_{*\Delta}$
 317 and $w_{*\Delta}$ are defined as the short sides of the horizontal triangle leaf, which are very
 318 easy to acquire in the computer scene. The three sides of a triangular leaf under
 319 varying leaf inclination angle are

320 $s_1 = \cos \theta_l (0.5 \times l_{*\Delta}) + \sin \theta_l \times l_{*\Delta}$ (C-19)

321 $s_2 = \cos \theta_l (0.5 \times w_{*\Delta}) + \sin \theta_l \times w_{*\Delta}$ (C-20)

322 $s_3 = \cos \theta_l \left(0.5 \times \sqrt{w_{*\Delta}^2 + l_{*\Delta}^2} \right) + \sin \theta_l \times \sqrt{w_{*\Delta}^2 + l_{*\Delta}^2}$ (C-21)

323 the canopy dimension parameter (leaf curvature is not considered) is

$$\begin{aligned}
l_L^* = l_{L\Delta} h &= \frac{\sum_{i=1}^{n_\Delta} h \left(\frac{\mathcal{G}_1}{\mathcal{G}_1 + \mathcal{G}_2 + \mathcal{G}_3} s_1 + \frac{\mathcal{G}_2}{\mathcal{G}_1 + \mathcal{G}_2 + \mathcal{G}_3} s_2 + \frac{\mathcal{G}_3}{\mathcal{G}_1 + \mathcal{G}_2 + \mathcal{G}_3} s_3 \right)}{n_\Delta} \\
&= \frac{\sum_{i=1}^{n_\Delta} h (0.5 \cos \theta_i + \sin \theta_i) \left(\mathcal{G}_1 l_{*\Delta} + \mathcal{G}_2 w_{*\Delta} + \mathcal{G}_3 \sqrt{w_{*\Delta}^2 + l_{*\Delta}^2} \right)}{n_\Delta (\mathcal{G}_1 + \mathcal{G}_2 + \mathcal{G}_3)}
\end{aligned} \tag{C-22}$$

Here $l_{L\Delta}$ is the length of the visible line in the triangular leaf, \mathcal{G}_1 , \mathcal{G}_2 and \mathcal{G}_3 are the random number from 0 to 1, n_Δ is the number of triangular leaves, and is easy to count in computer scene. $\frac{\mathcal{G}_1}{\mathcal{G}_1 + \mathcal{G}_2 + \mathcal{G}_3}$, $\frac{\mathcal{G}_2}{\mathcal{G}_1 + \mathcal{G}_2 + \mathcal{G}_3}$ and $\frac{\mathcal{G}_3}{\mathcal{G}_1 + \mathcal{G}_2 + \mathcal{G}_3}$ are the random probability of triangular edges.

D. Solving of the DRFs on the boundary of the canopy closure

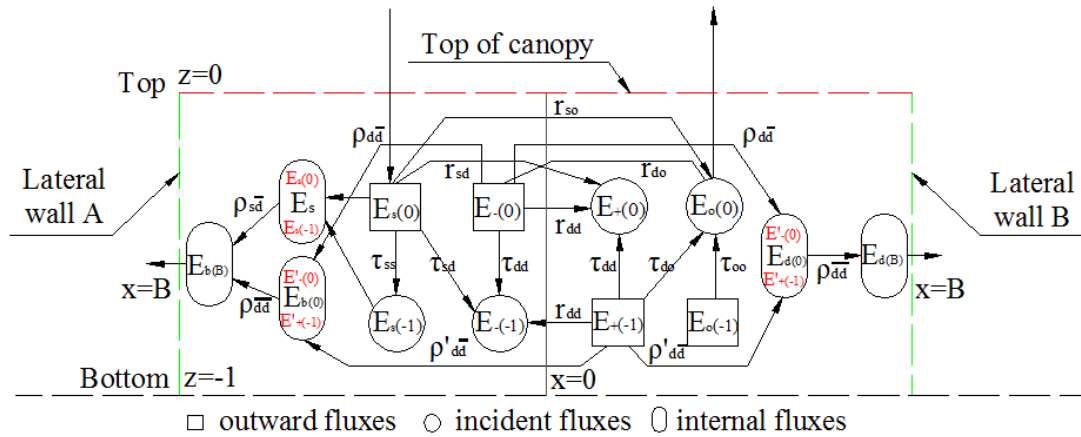
D-1 Construction of the layer scattering matrix

The boundary conditions (i.e., $z=0$, $z=-1$ and $x=B$ in Fig. B-3(b)) are considered, Eqs. (6-11) in the main text become scattering matrix in the canopy closure, and it is

$$\begin{aligned}
\begin{bmatrix} E_s(-1) \\ E_-(-1) \\ E_+(0) \\ E_o(0) \\ E_b(B) \\ E_d(B) \end{bmatrix} &= \begin{bmatrix} \tau_{ss} & 0 & 0 & 0 & 0 & 0 \\ \tau_{sd} & \tau_{dd} & r_{dd} & 0 & 0 & 0 \\ r_{sd} & r_{dd} & \tau_{dd} & 0 & 0 & 0 \\ r_{so} & r_{do} & \tau_{do} & \tau_{oo} & 0 & 0 \\ \rho_{s\bar{d}} & \rho_{d\bar{d}} & \rho'_{d\bar{d}} & \rho_{\bar{d}\bar{d}} & 0 & 0 \\ 0 & \rho_{d\bar{d}} & \rho'_{d\bar{d}} & \rho_{\bar{d}\bar{d}} & 0 & 0 \end{bmatrix} \begin{bmatrix} E_s(0) \\ E_-(0) \\ E_+(-1) \\ E_o(-1) \\ E_b(0) \\ E_d(0) \end{bmatrix}
\end{aligned} \tag{D-1}$$

r in Eq. (D-1) is reflectance factors in the homogeneous scattering layer, τ in Eq. (D-1) is transmittance factors in the homogeneous scattering layer, and they are derived from the four-stream radiation transfer theory (pers. comm. W. Verhoef, 2018).

338 ρ is radiative transfer ratio in the homogeneous scattering layer (the specific
339 derivation is detailed in D-2 in this section). Their subscripts represent the properties
340 of incident and outgoing radiation, and can be summarized by the follows: s
341 represents specular flux in direction of direct solar radiation; o represents specular
342 flux in direct viewing direction; d represents diffuse flux of the vertical hemisphere;
343 \bar{d} represents diffuse flux of the horizontal hemisphere. These parameters describe the
344 theory for bidirectional reflectance distribution Function (BRDF) inside the canopy
345 closure. Eq. (D-1) is changed into the notation of matrix-vector, there is $\Phi_{out} = \mathbf{S}\Phi_{in}$,
346 in which \mathbf{S} is the layer scattering matrix for the specular and diffuse fluxes. The
347 relationship of the sources and sinks in the radiative transfer of specular and diffuse
348 flux within the canopy closure is illustrated in Fig. D-1.



349 Fig. D-1 Interactions of fluxes for an isolated homogeneous scattering layer in canopy
350 closure of row planted crops.
351

352 D-2 Derivation of the radiative transfer ratio

353 For the diffuse flux vectors in the vertical direction (i.e., E_- and E_+), the
354 system of the differential equation is

$$355 \quad \frac{d}{L'dz} \begin{bmatrix} E_- \\ E_+ \end{bmatrix} = \begin{bmatrix} a & -\sigma \\ \sigma & -a \end{bmatrix} \begin{bmatrix} E_- \\ E_+ \end{bmatrix} \quad (\text{D-2})$$

356 This equation is diagonalized, and its eigenvalues and eigenvectors are

$$357 \quad \mathbf{\Lambda}_{dd} = \begin{bmatrix} m & 0 \\ 0 & -m \end{bmatrix}, \quad \mathbf{P}_{dd} = \begin{bmatrix} 1 & \frac{a-m}{\sigma} \\ \frac{\sigma}{a+m} & 1 \end{bmatrix} \quad (\text{D-3})$$

358 For the horizontal diffuse flux, the system of the differential equation is

$$359 \quad \frac{d}{Udz} \begin{bmatrix} E_b \\ E_d \end{bmatrix} = \begin{bmatrix} g & g' \\ g & g' \end{bmatrix} \begin{bmatrix} E_- \\ E_+ \end{bmatrix} \quad (\text{D-4})$$

360 Eq. (D-4) is diagonalized, and its eigenvalues and eigenvectors are

$$361 \quad \mathbf{\Lambda}_{hdd} = \begin{bmatrix} 0 & 0 \\ 0 & g + g' \end{bmatrix}, \quad \mathbf{P}_{hdd} = \begin{bmatrix} -g' & 1 \\ g & 1 \end{bmatrix} \quad (\text{D-5})$$

362 In matrix analysis and geometry, the eigenvector is the basis of the matrix, which

363 determines the direction of the matrix. Therefore, the eigenvector is used in the

364 calculation. For Eqs. (D, 3 and 5), there are the following relationships

$$365 \quad \begin{bmatrix} \rho_{d\bar{d}} + \delta_1 & \rho'_{d\bar{d}} + \delta_2 \\ \rho_{d\bar{d}} + \delta_1 & \rho'_{d\bar{d}} + \delta_2 \end{bmatrix} = \begin{bmatrix} 1 & \frac{a-m}{\sigma} \\ \frac{\sigma}{a+m} & 1 \end{bmatrix}^{-1} \begin{bmatrix} -g' & 1 \\ g & 1 \end{bmatrix} \quad (\text{D-6})$$

$$= \begin{bmatrix} 1 & r_\infty \\ r_\infty & 1 \end{bmatrix}^{-1} \begin{bmatrix} -g' & 1 \\ g & 1 \end{bmatrix} = \begin{bmatrix} \frac{g' + gr_\infty}{1 - r_\infty^2} & \frac{g'r_\infty + g}{1 - r_\infty^2} \\ \frac{r_\infty - 1}{1 - r_\infty^2} & \frac{1 - r_\infty}{1 - r_\infty^2} \end{bmatrix}$$

366 the infinite reflectance is defined as $r_\infty = \frac{a-m}{\sigma} = \frac{\sigma}{a+m}$ [11]. $\rho_{d\bar{d}}$ is the radiative

367 transfer ratio from downward diffuse to the lateral “wall”. $\rho'_{d\bar{d}}$ is the radiative

368 transfer ratio from upward diffuse to the lateral “wall”. δ_1 and δ_2 are

369 cross-radiation coefficient for $\rho_{d\bar{d}}$ and $\rho'_{d\bar{d}}$, respectively. There are two pairs of

370 solutions for Eq. (D-6). $\frac{r_\infty - 1}{1 - r_\infty^2}$ is overflowing, and the downside-solutions of the

371 matrix is omitted. Therefore, only upside-solutions of the matrix are used

$$372 \quad \rho_{d\bar{d}} + \delta_1 = \frac{g' + gr_\infty}{1 - r_\infty^2} \quad (\text{D-7})$$

$$373 \quad \rho'_{d\bar{d}} + \delta_2 = \frac{g'r_\infty + g}{1 - r_\infty^2} \quad (\text{D-8})$$

374 then

$$375 \quad \rho_{d\bar{d}} + \delta_1 = \left\{ \frac{g'}{1 - r_\infty^2} + \frac{gr_\infty}{1 - r_\infty^2} \right\} \approx gr_\infty [1 + r_\infty + r_\infty^2 \dots] + g' [1 + r_\infty + r_\infty^2 \dots] \quad (\text{D-9})$$

$$376 \quad \rho'_{d\bar{d}} + \delta_2 = \left[\frac{g'r_\infty}{1 - r_\infty^2} + \frac{g}{1 - r_\infty^2} \right] \approx g'r_\infty [1 + r_\infty + r_\infty^2 \dots] + g [1 + r_\infty + r_\infty^2 \dots] \quad (\text{D-10})$$

377 Here

$$378 \quad \delta_1 = g' [1 + r_\infty + r_\infty^2 \dots] \quad (\text{D-11})$$

$$379 \quad \delta_2 = g [1 + r_\infty + r_\infty^2 \dots] \quad (\text{D-12})$$

380 Therefore, there are

$$381 \quad \rho_{d\bar{d}} = gr_\infty [1 + r_\infty + r_\infty^2 \dots] \approx \frac{gr_\infty}{1 - r_\infty^2} \quad (\text{D-13})$$

$$382 \quad \rho'_{d\bar{d}} = g'r_\infty [1 + r_\infty + r_\infty^2 \dots] \approx \frac{g'r_\infty}{1 - r_\infty^2} \quad (\text{D-14})$$

383 In Eqs. (D, 13-14), the conversion factor is multiplied by the infinite reflectance from

384 one interaction to n interactions, which more satisfies the physical meaning.

385 Superposition principle (mathematical physics) [12] is used to decompose the

386 radiation field, and there is a physical relationship for the diffuse horizontal

387 hemispheric flux density through the lateral “wall” A

388 $E_b(B) = \int_{-1}^0 E_b(B, z) dz = \int_{-1}^0 e^{Um'z} E_s(0, z) dz = e^{Um'z} E_s(0, z) \Big|_{-1}^0 = E_s(0) (1 - e^{-Um'})$ (D-15)

389 Here $\frac{dE_b(B, z)}{Udz} \approx m'E_b(0, z) \Rightarrow E_b(B, z) = e^{Um'z} E_b(0, z)$. The radiative transfer ratio

390 of directional horizontal hemispherical direction is

391 $\rho_{\bar{d}\bar{d}} = 1 - e^{-Um'}$ (D-16)

392 similarly, the radiative transfer ratio of horizontal bi-hemispherical direction is

393 $\rho_{\bar{d}\bar{d}} = 1 - e^{-Um'}$ (D-17)

394 **D-3 Solving of DRFs on the boundary of the canopy closure**

395 The block matrices are used to calculate the DRF. They are

396 $\mathbf{E}^d = \begin{bmatrix} E_s \\ E_- \end{bmatrix}, \mathbf{E}^u = \begin{bmatrix} E_+ \\ E_o \end{bmatrix}, \mathbf{E}^e = \begin{bmatrix} E_b \\ E_d \end{bmatrix},$

397 $\mathbf{T}_d = \begin{bmatrix} \tau_{ss} & 0 \\ \tau_{sd} & \tau_{dd} \end{bmatrix}, \mathbf{R}_b = \begin{bmatrix} 0 & 0 \\ r_{dd} & 0 \end{bmatrix}, \mathbf{R}_t = \begin{bmatrix} r_{sd} & r_{dd} \\ r_{so} & r_{do} \end{bmatrix},$

398 $\mathbf{T}_u = \begin{bmatrix} \tau_{dd} & 0 \\ \tau_{do} & \tau_{oo} \end{bmatrix}, \mathbf{H}_{bl} = \begin{bmatrix} \rho_{s\bar{d}} & \rho_{d\bar{d}} \\ 0 & \rho_{d\bar{d}} \end{bmatrix}, \mathbf{H}_{da} = \begin{bmatrix} \rho'_{d\bar{d}} & \rho_{\bar{d}\bar{d}} \\ \rho'_{d\bar{d}} & \rho_{\bar{d}\bar{d}} \end{bmatrix}$ (D-18)

399 Then, Eq. (D-1) is simplified as

400 $\begin{bmatrix} \mathbf{E}^d(b) \\ \mathbf{E}^u(t) \\ \mathbf{E}^e(s) \end{bmatrix} = \begin{bmatrix} \mathbf{T}_d & \mathbf{R}_b & 0 \\ \mathbf{R}_t & \mathbf{T}_u & 0 \\ \mathbf{H}_{bl} & \mathbf{H}_{da} & 0 \end{bmatrix} \begin{bmatrix} \mathbf{E}^d(t) \\ \mathbf{E}^u(b) \\ \mathbf{E}^e(i) \end{bmatrix}$ (D-19)

401 in which the indices refer to the bottom of the canopy in the vertical direction (b),

402 top of the canopy in the vertical direction (t), inner part of the canopy in the

403 horizontal direction (i), surface of the canopy in the horizontal direction (s),

404 downward direction (d), upward direction (u), horizontal direction in lateral “wall”

405 A (bl), and horizontal direction in lateral “wall” B (da).

406 For a non-Lambert surface, there is

$$407 \quad \mathbf{E}^u(b) = \mathbf{R}_s \mathbf{E}^d(b) \quad (\text{D-20})$$

408 Defining \mathbf{R}_s as the matrix of the non-Lambert reflectance factor of soil, there is

$$409 \quad \mathbf{R}_s = \begin{bmatrix} r_{sd}^s & r_{dd}^s \\ r_{so}^s & r_{do}^s \end{bmatrix}. \text{ Then, the relationship between } \mathbf{E}^u(t) \text{ and } \mathbf{E}^d(t) \text{ can be}$$

410 expressed as

$$411 \quad \mathbf{E}^u(t) = \mathbf{R}_\perp \mathbf{E}^d(t) \quad (\text{D-21})$$

412 where \mathbf{R}_\perp is the matrix of the reflectance factors at the top surface of the canopy,

413 and

$$414 \quad \mathbf{R}_\perp = \mathbf{R}_t + \mathbf{T}_u (\mathbf{I} - \mathbf{R}_s \mathbf{R}_b)^{-1} \mathbf{R}_s \mathbf{T}_d \quad (\text{D-22})$$

$$415 \quad \text{Here each element in } \mathbf{R}_\perp \text{ is } \mathbf{R}_\perp = \begin{bmatrix} r_{sd}^* & r_{dd}^* \\ r_{so}^* & r_{do}^* \end{bmatrix}.$$

416 a) The DRF at the top of canopy closure

417 According to the DRF of the top of canopy derived from the original four-stream

418 radiative transfer equations, i.e., $R = \frac{r_{so}^* E_s(0) + r_{do}^* E_-(0)}{E_s(0) + E_-(0)}$ in [11], here $E_s(0)$ is the

419 specular flux on top of canopy and $E_-(0)$ is the diffuse flux on top of canopy. From

420 this equation, the bi-directional reflectance factor (r_{so}^*) and the

421 hemispherical-directional reflectance factor (r_{do}^*) need to be calculated. [1] gives the

422 result of a derivation of Eq. (D-22):

$$423 \quad r_{so}^* = r_{so} + \tau_{ss} \tau_{oo} r_s + \left\{ [(\tau_{ss} + \tau_{sd}) \tau_{do} + (\tau_{sd} + \tau_{ss} r_s r_{dd}) \tau_{oo}] \frac{1}{1 - r_s r_{dd}} \right\} r_s \quad (\text{D-23})$$

$$424 \quad r_{do}^* = r_{do} + \left[(\tau_{do} + \tau_{oo}) \tau_{dd} \frac{1}{1 - r_s r_{dd}} \right] r_s \quad (\text{D-24})$$

425 According to (pers. comm. W. Verhoef, 2018), r_{so} in Eq. (D-23) is bidirectional
 426 reflectance in the layer, and it consists of the single-scattering of specular flux in the
 427 layer (r_{so}^1) and the multiple-scattering of specular flux in the layer (r_{so}^m). The
 428 single-scattering of specular flux in the canopy, and its is

$$429 \quad r_{so}^1 = wL'S \quad (D-25)$$

430 we consider the row structure effect to modify the row structure on the differential
 431 leaf area index (leaf area density) for canopy in the vertical direction of continuous
 432 crops (L') and area fractions of canopy (S), Eq. (D-25) is modified, then the
 433 single-scattering of specular flux in the canopy closure ($r_{so_v}^1$) is

$$434 \quad r_{so_v}^1 = wL'_{row}S_{closure_s}(z) \quad (D-26)$$

435 Here L'_{row} and $S_{closure_s}(z)$ are parameters after considering the influence of the row
 436 structure on the canopy closure (Table C-1). L'_{row} is the differential leaf area index
 437 (leaf area density) for canopy closure in the vertical direction, and
 438 $L'_{row} = (A_1 + A_2) Lf(\theta_l) d\theta_l / A_1 h$. Similarly, the multiple-scattering of specular flux in
 439 the canopy closure is

$$440 \quad r_{so_v}^m = S_{closure_d} \left[\frac{(v + v'r_\infty)T_1 + (r_\infty v + v')T_2}{1 - r_\infty^2} \right. \quad (D-27)$$

$$\left. - (Q_v \quad P_v) \left[\begin{array}{cc} 1 & r_\infty e^{-mL_{row}\Omega_E} \\ r_\infty e^{-mL_{row}\Omega_E} & 1 \end{array} \right]^{-1} \begin{pmatrix} Q_s \\ P_s \end{pmatrix} r_\infty / (1 - r_\infty^2) \right]$$

441 Here T_1 , T_1 , Q_v , Q_s , P_v and P_s are functions derived from four-stream radiative
 442 transfer theory (pers. comm. W. Verhoef, 2018). According to [1], $\tau_{ss}\tau_{oo}r_s$ in Eq.
 443 (D-23) is the single-scattering of specular flux from the soil in the canopy, and we
 444 consider the row structure with reference to Eq.(D-26), the single-scattering of
 445 specular flux from the soil in the canopy closure ($r_{so_s}^1$) is

446 $r_{so_s}^1 = S_{closure_s}(h)r_s$ (D-28)

447 According to [1], $\left\{ \left[(\tau_{ss} + \tau_{sd})\tau_{do} + (\tau_{sd} + \tau_{ss}r_s r_{dd})\tau_{oo} \right] \frac{1}{1 - r_s r_{dd}} \right\} r_s$ in Eq. (D-23) is

448 multiple-scattering between soil and vegetation in the canopy for specular flux.

449 Similar to the modification of row structure in Eq. (D-26), the multiple-scattering

450 between soil and vegetation in the canopy closure for specular flux is

451 $r_{so_s}^m = (S_{closure_d}r_s) \left\{ \left[(\tau_{ss} + \tau_{sd})\tau_{do} + (\tau_{sd} + \tau_{ss}r_s r_{dd})\tau_{oo} \right] \frac{1}{1 - r_s r_{dd}} \right\}$ (D-29)

452 According to [1], r_{do} in Eq. (D-24) is the single-scattering of diffuse flux in the

453 canopy. Similar to the previous modification of row structure, the single-scattering of

454 diffuse flux in the canopy closure is

455 $r_{do}^1 = r_{do} S_{closure_d}$ (D-30)

456 According to [1], $\left[(\tau_{do} + \tau_{oo})\tau_{dd} \frac{1}{1 - r_s r_{dd}} \right] r_s$ in Eq. (D-24) is the multiple-scattering

457 of diffuse flux in the canopy. Similar to the modification of row structure in Eq.

458 (D-26), the multiple-scattering of diffuse flux in the canopy closure is

459 $r_{do}^m = S_{closure_d} \left[(\tau_{do} + \tau_{oo})\tau_{dd} \frac{1}{1 - r_s r_{dd}} \right] r_s$ (D-31)

460 According to Eqs. (D, 26 and 28), the bi-directional reflectance factor for

461 single-scattering of specular flux ($r_{so_c_1}^*$) is

462 $r_{so_1}^* = r_{so_v}^1 + r_{so_s}^1$
 $= wL'_{row} S_{closure_s}(z) + S_{closure_s}(h)r_s$ (D-32)

463 According to Eqs. (D, 27 and 29), the bi-directional reflectance factor for

464 multiple-scattering of specular flux ($r_{so_c_m}^*$) is

$$\begin{aligned}
r_{so_m}^* &= r_{so_v}^m + r_{so_s}^m \\
465 \quad &= S_{closure_d} \left[\begin{array}{c} \frac{(v + v'r_\infty)T_1 + (r_\infty v + v')T_2}{1 - r_\infty^2} \\ - \begin{pmatrix} Q_v & P_v \end{pmatrix} \begin{bmatrix} 1 & r_\infty e^{-mL'_{row}\Omega_E} \\ r_\infty e^{-mL'_{row}\Omega_E} & 1 \end{bmatrix}^{-1} \begin{pmatrix} Q_s \\ P_s \end{pmatrix} r_\infty / (1 - r_\infty^2) \end{array} \right] \\
&+ \left(S_{closure_d} r_s \right) \left\{ \left[(\tau_{ss} + \tau_{sd})\tau_{do} + (\tau_{sd} + \tau_{ss}r_s r_{dd})\tau_{oo} \right] \frac{1}{1 - r_s r_{dd}} \right\}
\end{aligned} \tag{D-33}$$

466 According to Eqs. (D, 30 and 31), the hemispherical-directional reflectance factor
467 (this physical quantity describes diffuse flux) ($r_{do_c}^*$) is

$$\begin{aligned}
468 \quad r_{do}^* &= r_{do}^1 + r_{do}^m \\
&= S_{closure_d} \left\{ r_{do} + \left[(\tau_{do} + \tau_{oo})\tau_{dd} \frac{1}{1 - r_s r_{dd}} \right] r_s \right\}
\end{aligned} \tag{D-34}$$

469 According to the DRF at the top of canopy derived from the original four-stream
470 radiative transfer equations, i.e., $R = \frac{r_{so}^* E_s(0) + r_{do}^* E_-(0)}{E_s(0) + E_-(0)}$ in [11], the nature of the
471 incident radiant flux is considered, i.e., specular flux and diffuse flux. The
472 single-scattering of the canopy closure (R_{c_1}) is

$$473 \quad R_{c_1} = \frac{r_{so_1}^* E_s(0)}{E_s(0) + E_-(0)} \tag{D-35}$$

474 and the multiple-scattering of the canopy closure (R_{c_m}) is

$$475 \quad R_{c_m} = \frac{r_{so_m}^* E_s(0) + r_{do}^* E_-(0)}{E_s(0) + E_-(0)} \tag{D-36}$$

476 **Note:** $r_{so_1}^*$, $r_{so_m}^*$, and r_{do}^* are $r_{so_c_1}^*$, $r_{so_c_m}^*$, and $r_{do_c}^*$ in the text. To distinguish
477 them from reflectance factor of between-row, hence, a c is added to the subscript in
478 the mian text .

479 **b) The DRF of lateral “wall” A and the DRF of lateral “wall”**

480 **B**

481 Combining Eqs. (D, 4-6), there are

$$482 \quad \mathbf{E}^e(s) = \left[\mathbf{H}_{bl} \mathbf{R}_\perp^{-1} + \mathbf{H}_{da} \mathbf{T}_u^{-1} (\mathbf{I} - \mathbf{R}_l \mathbf{R}_\perp^{-1}) \right] \mathbf{E}^u(t) \quad (\text{D-37})$$

$$483 \quad \mathbf{E}^e(s) = \left[\mathbf{H}_{bl} \mathbf{R}_s^{-1} \mathbf{T}_d^{-1} (\mathbf{I} - \mathbf{R}_b \mathbf{R}_s) + \mathbf{H}_{da} \right] \mathbf{E}^u(b) \quad (\text{D-38})$$

484 We define \mathbf{G}_1 as the ratio matrix of the radiative transfer from the top surface to

485 the lateral “wall” of the canopy closure, and \mathbf{G}_2 as the ratio matrix of the radiative

486 transfer from the bottom surface to the lateral “wall” of the canopy closure, namely

$$487 \quad \mathbf{G}_1 = \begin{bmatrix} g_{s\bar{d}} & g_{d\bar{d}} \\ g_{so} & g_{\bar{d}o} \end{bmatrix} = \mathbf{H}_{bl} \mathbf{R}_\perp^{-1} + \mathbf{H}_{da} \mathbf{T}_u^{-1} (\mathbf{I} - \mathbf{R}_l \mathbf{R}_\perp^{-1}) \quad (\text{D-39})$$

$$488 \quad \mathbf{G}_2 = \begin{bmatrix} g'_{s\bar{d}} & g'_{d\bar{d}} \\ g'_{so} & g'_{\bar{d}o} \end{bmatrix} = \mathbf{H}_{bl} \mathbf{R}_s^{-1} \mathbf{T}_d^{-1} (\mathbf{I} - \mathbf{R}_b \mathbf{R}_s) + \mathbf{H}_{da} \quad (\text{D-40})$$

489 Combining with Eqs. (D, 4-6), there are

$$490 \quad \mathbf{E}^e(s) = \mathbf{G}_1 \mathbf{E}^u(t) \quad (\text{D-41})$$

$$491 \quad \mathbf{E}^e(s) = \mathbf{G}_2 \mathbf{E}^u(b) \quad (\text{D-42})$$

492 Then, multiplying Eq. (D-41) by $\mathbf{E}^d(t)^{-1}$ produces

$$493 \quad \mathbf{E}^e(s) \times \mathbf{E}^d(t)^{-1} = \mathbf{G}_1 \mathbf{E}^u(t) \times \mathbf{E}^d(t)^{-1} = \mathbf{G}_1 \mathbf{R}_\perp \quad (\text{D-43})$$

494 where \times denotes the vector product.

495 Combining Eqs. (B, 17-18), Eq. (D-42), and Eq. (D-43), Eqs. (D, 41-42) can be

496 written as

$$497 \quad \frac{1}{o_1} \mathbf{E}^e(s) \times \mathbf{E}'_-(*)^{-1} = \mathbf{G}_1 \mathbf{R}_\perp \quad (\text{D-44})$$

$$498 \quad \frac{1}{o_2} \mathbf{E}^e(s) \times \mathbf{E}'_+(*)^{-1} = \mathbf{G}_2 \quad (\text{D-45})$$

499 where $\mathbf{E}'_-(*)$ and $\mathbf{E}'_+(*)$ are the vectors of the downward diffuse flux and

500 upward diffuse flux in the diagonal area of the canopy closure, respectively, as shown
 501 in Fig. B-2. The symbol * represents the diagonal area. The sum of Eq. (D-44) and
 502 Eq. (D-45) is

$$503 \quad \mathbf{E}^e(s)^{-1} \times \mathbf{E}'_-(*) + \mathbf{E}^e(s)^{-1} \times \mathbf{E}'_+ (*) = (\mathbf{G}_1 \mathbf{R}_\perp o_1)^{-1} + (\mathbf{G}_2 o_2)^{-1} \quad (\text{D-46})$$

504 Eq. (B-45) is resolved as

$$505 \quad [\mathbf{E}'_-(*) + \mathbf{E}'_+ (*)] \times \mathbf{E}^e(s)^{-1} = (\mathbf{G}_1 \mathbf{R}_\perp o_1)^{-1} + (\mathbf{G}_2 o_2)^{-1} \quad (\text{D-47})$$

506 Combined with Eq. (B-19), there is $\mathbf{E}^e(i) = [\mathbf{E}'_+ (*) + \mathbf{E}'_-(*)] o_3$. Then, Eq. (D-47)
 507 becomes

$$508 \quad \begin{aligned} \mathbf{R}_\parallel &= \mathbf{E}^e(s) \times \mathbf{E}^e(i)^{-1} = \left[(\mathbf{G}_1 \mathbf{R}_\perp o_1)^{-1} + (\mathbf{G}_2 o_2)^{-1} \right]^{-1} o_3^{-1} \\ &= \mathbf{G}_1 \mathbf{R}_\perp o_1 \mathbf{G}_2 o_2 [\mathbf{G}_1 \mathbf{R}_\perp o_1 + \mathbf{G}_2 o_2]^{-1} o_3^{-1} = \begin{bmatrix} r_{\parallel s\bar{d}} & r_{\parallel d\bar{d}} \\ r_{\parallel s\bar{o}} & r_{\parallel \bar{d}o} \end{bmatrix} \end{aligned} \quad (\text{D-48})$$

509 where \mathbf{R}_\parallel is the matrix of horizontal transmittance factor in the lateral “wall”. Here,
 510 the soil is assumed to be Lambertian, namely $r_{sd}^s = r_{dd}^s = r_{so}^s = r_{do}^s = r_s$, and the
 511 elements of \mathbf{R}_\parallel are

$$512 \quad r_{\parallel s\bar{d}} = \frac{o_1 o_2 \rho'_{d\bar{d}} (D_1 + \tau_{dd} \rho_{s\bar{d}} \tau_{oo})}{o_3 (M_1 + o_1 \tau_{dd} \rho_{s\bar{d}} \tau_{oo})} \quad (\text{D-49})$$

$$513 \quad r_{\parallel d\bar{d}} = \frac{o_1 o_2 \rho_{d\bar{d}} (D_1 + \tau_{dd} \rho_{s\bar{d}} \tau_{oo})}{o_3 M_2} \quad (\text{D-50})$$

$$514 \quad r_{\parallel s\bar{o}} = \frac{o_1 o_2 \rho'_{d\bar{d}} D_1}{o_3 M_1} \quad (\text{D-51})$$

$$515 \quad r_{\parallel \bar{d}o} = \frac{o_1 o_2 \rho_{d\bar{d}} D_1}{o_3 M_2} \quad (\text{D-52})$$

516 in which

$$517 \quad \begin{aligned} D_1 &= \rho_{d\bar{d}} r_{dd} \tau_{do} - \rho_{d\bar{d}} r_{do} \tau_{dd} - \rho_{d\bar{d}} r_{dd}^* \tau_{do} + \rho_{d\bar{d}} r_{do}^* \tau_{dd} - \rho'_{d\bar{d}} r_{dd} \tau_{oo} + \rho_{d\bar{d}} r_{sd} \tau_{do} \\ &- \rho_{d\bar{d}} r_{so} \tau_{dd} - \rho_{d\bar{d}} r_{sd}^* \tau_{do} + \rho_{d\bar{d}} r_{so} \tau_{dd} - \rho'_{d\bar{d}} r_{sd} \tau_{oo} + \rho'_{d\bar{d}} r_{sd}^* \tau_{oo} + \rho_{d\bar{d}} \tau_{dd} \tau_{oo} \end{aligned} \quad (\text{D-53})$$

$$\begin{aligned}
518 \quad M_1 &= o_1 \rho_{\bar{d}\bar{d}} r_{sd} \tau_{do} - o_1 \rho_{\bar{d}\bar{d}} r_{so} \tau_{dd} - o_1 \rho_{\bar{d}\bar{d}} r_{sd}^* \tau_{do} + o_1 \rho_{\bar{d}\bar{d}} r_{so}^* \tau_{dd} \\
&- o_1 \rho'_{\bar{d}\bar{d}} r_{sd} \tau_{oo} + o_1 \rho'_{\bar{d}\bar{d}} r_{sd}^* \tau_{oo} + o_2 \rho'_{\bar{d}\bar{d}} \tau_{dd} \tau_{oo}
\end{aligned} \tag{D-54}$$

$$\begin{aligned}
519 \quad M_2 &= o_1 \rho_{\bar{d}\bar{d}} r_{dd} \tau_{do} - o_1 \rho_{\bar{d}\bar{d}} r_{do} \tau_{dd} - o_1 \rho_{\bar{d}\bar{d}} r_{dd}^* \tau_{do} + o_1 \rho_{\bar{d}\bar{d}} r_{so}^* \tau_{dd} - o_1 \rho'_{\bar{d}\bar{d}} r_{dd} \tau_{oo} \\
&+ o_1 \rho'_{\bar{d}\bar{d}} r_{dd}^* \tau_{oo} + o_2 \rho_{\bar{d}\bar{d}} \tau_{dd} \tau_{oo} + o_1 \rho_{\bar{d}\bar{d}} \tau_{dd} \tau_{oo}
\end{aligned} \tag{D-55}$$

520 According to DRF derived from the original four-stream radiative transfer equations,

$$521 \quad \text{i.e., } R = \frac{r_{so}^* E_s(0) + r_{do}^* E_-(0)}{E_s(0) + E_-(0)} \text{ in [11], this equation shows that the DRF is the ratio of the}$$

522 reflected flux ($r_{so}^* E_s(0) + r_{do}^* E_-(0)$) to the incident flux ($E_s(0) + E_-(0)$) at the top of

523 the canopy. Similarly, we need to calculate incident flux in the lateral “wall”. Incident

524 flux in the lateral “wall” includes specular flux and diffuse flux. The specular flux in

525 surface of lateral “wall” is

$$526 \quad E_{\parallel s}(B) = \rho_{s\bar{d}} E_s(0) \tag{D-56}$$

527 and the diffuse flux in surface of lateral “wall” is

$$\begin{aligned}
528 \quad E_{\parallel \pm}(B) &= \rho_{d\bar{d}} E_-(0) + \rho'_{d\bar{d}} E_+(-1) = \rho_{d\bar{d}} E_-(0) + \rho'_{d\bar{d}} \{ [E_-(-1) + E_s(-1)] r_s \} \\
&= \rho_{d\bar{d}} E_-(0) + \rho'_{d\bar{d}} \{ [e^{-L_{\text{row}}} E_-(0) + e^{-kL_{\text{row}}} E_s(0)] r_s \}
\end{aligned} \tag{D-57}$$

529 Finally, DRF of the lateral “wall” A is

$$530 \quad R_b = \frac{r_{\parallel s\bar{d}} E_{\parallel s}(B) + r_{\parallel d\bar{o}} E_{\parallel \pm}(B)}{E_{\parallel s}(B) + E_{\parallel \pm}(B)} \tag{D-58}$$

531 and the DRF of the lateral “wall” B is

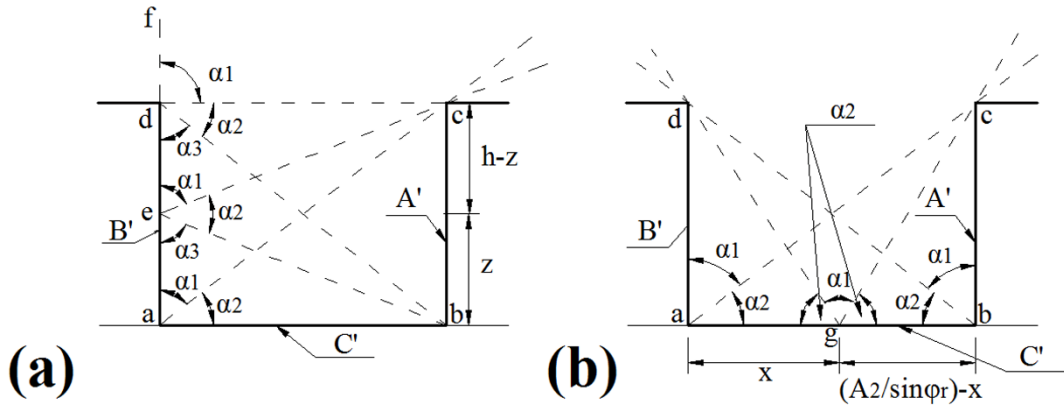
$$532 \quad R_d = \frac{r_{\parallel d\bar{o}} E_{\parallel s}(B) + r_{\parallel d\bar{d}} E_{\parallel \pm}(B)}{E_{\parallel s}(B) + E_{\parallel \pm}(B)} \tag{D-59}$$

533 **E. Solving of the DRF of between-row based**
534 **on integral radiative transfer equation**

535 The between-row area consists of two lateral “walls” (A' and B'),
536 between-row background (C') and escaping surface ($abcd$ in Fig. E-1). Radiation
537 transfer in this area is influenced by two mediums, i.e., vegetation leaf and soil
538 particle. The differential-integral form of the radiative transfer equation is transformed
539 into an integral form to describe the radiative transfer among these four components
540 [13], there is

541
$$f(z, \Omega) = \int_{4\pi} \mathbf{K}(x, z, \Omega' \rightarrow \Omega) f(z, \Omega') d\Omega + f_0(z, \Omega) \quad (\text{E-1})$$

542 Here $f_0(z, \Omega)$ is the source function of a medium. $\mathbf{K}(x, z, \Omega' \rightarrow \Omega)$ is the transfer
543 probability of collision, and $\mathbf{K}(x, z, \Omega' \rightarrow \Omega) = \mathbf{k}(x, z, \Omega' \rightarrow \Omega) * \mathbf{a}(x, z, \Omega' \rightarrow \Omega)$,
544 here $*$ is symbol of hadamard product. $\mathbf{k}(x, z, \Omega' \rightarrow \Omega)$ is the matrix of transfer
545 probabilities between lateral “walls”, between-row background and escaping surface,
546 which is composed of the probabilities of four components, and its expression
547 reference E-1 in this section. $\mathbf{a}(x, z, \Omega' \rightarrow \Omega)$ is the matrix of light attenuation
548 coefficients, and its expression reference E-2 in this section. Finally, the equation is
549 solved in E-3 in this section.



550

551 Fig. E-1 Sketch of transfer probability matrix in the between-row area. (a) Transfer probability
552 matrix in the Z-axis; (b) transfer probability matrix in the X-axis.

553 E-1 Transfer probability

554 According to Fig. E-1, when the value of the solar azimuth angle is
555 $0^\circ \leq \phi_s < 180^\circ$, B' is the lateral “wall” A. Similarly, when the value of the solar
556 azimuth angle is $180^\circ \leq \phi_s < 360^\circ$, A' is the lateral “wall” A. The related angles are
557 shown in Fig. E-1, α_1 is the angle of radiation escaping in the between-row, α_2 is the
558 angle of radiative transfer between both lateral “walls” in the between-row, α_3 is the
559 angle of radiative transfer between lateral “wall” and soil background in the
560 between-row. The transfer probability in the between-row is the ratio of these angles
561 to the sum angle. Therefore, the average probability of radiation escaping from the

562 lateral “wall” ($k_{B(A) \rightarrow}$) is $\frac{\angle fdc}{\pi} = 0.5$, $z = h$, $\frac{\angle fec}{\pi}$, $z \in (0, h)$, and

563 $\frac{2\angle fac}{\pi}$, $z = 0$. Then

$$\begin{aligned}
k_{B(A) \rightarrow A(B)} &= \frac{1}{h} \int_0^h P_{B(A) \rightarrow A(B)} dz, \\
564 \quad P_{B(A) \rightarrow A(B)} &= \begin{cases} \frac{1}{\pi} \arctan\left(\frac{h \sin \varphi_{or}}{A_2}\right) & z = h \\ \frac{1}{\pi} \left\{ \pi - \arctan\left[\frac{A_2}{\sin \varphi_{or} (h-z)}\right] - \arctan\left(\frac{A_2}{z \sin \varphi_{or}}\right) \right\} & z \in (0, h) \\ \frac{2}{\pi} \arctan\left(\frac{h \sin \varphi_{or}}{A_2}\right) & z = 0 \end{cases} \quad (E-2)
\end{aligned}$$

565 Eq. (E-2) is a linear decreasing function, in which $k_{B(A) \rightarrow}$ decreases with the
566 increase of the depth of canopy closure. Similarly, the average probability of radiation
567 transferring between two lateral “walls” is

$$\begin{aligned}
k_{B(A) \rightarrow A(B)} &= \frac{1}{h} \int_0^h P_{B(A) \rightarrow A(B)} dz, \\
568 \quad P_{B(A) \rightarrow A(B)} &= \begin{cases} \frac{1}{\pi} \arctan\left(\frac{h \sin \varphi_{or}}{A_2}\right) & z = h \\ \frac{1}{\pi} \left\{ \pi - \arctan\left[\frac{A_2}{\sin \varphi_{or} (h-z)}\right] - \arctan\left(\frac{A_2}{z \sin \varphi_{or}}\right) \right\} & z \in (0, h) \\ \frac{2}{\pi} \arctan\left(\frac{h \sin \varphi_{or}}{A_2}\right) & z = 0 \end{cases} \quad (E-3)
\end{aligned}$$

569 Eq. (E-3) is a hyperbolic function, in which $k_{B(A) \rightarrow A(B)}$ decreases first, then increases
570 with the increase of depth of canopy closure. The average probability of radiation
571 transferring from the lateral “wall” to between-row background is

$$\begin{aligned}
572 \quad k_{B(A) \rightarrow C} &= \frac{1}{h} \int_0^h P_{B(A) \rightarrow C} dz, \quad P_{B(A) \rightarrow C} = \begin{cases} \frac{1}{\pi} \arctan\left(\frac{A_2 h}{z \sin \varphi_{or}}\right) & z = h \\ \frac{1}{\pi} \arctan\left(\frac{A_2}{z \sin \varphi_{or}}\right) & z \in (0, h) \\ 0 & z = 0 \end{cases} \quad (E-4)
\end{aligned}$$

573 Eq. (E-4) is an incremental function with the increase of depth. Using the same
574 mathematical principles, the average probability of the radiation escaping from the
575 between-row background is

$$\begin{aligned}
k_{C \rightarrow} &= \frac{1}{A_2} \int_0^{A_2} P_{C \rightarrow} dx, \\
576 \quad P_{C \rightarrow} &= \begin{cases} \frac{2}{\pi} \arctan\left(\frac{A_2 h}{\sin \varphi_{or}}\right) & (x = A_2) \wedge (x = 0) \\ \frac{1}{\pi} \left[\pi - \arctan\left(\frac{h \sin \varphi_r}{A_2 - x \sin \varphi_{or}}\right) - \arctan\left(\frac{h}{x}\right) \right] & x \in (0, A_2) \end{cases} \quad (E-5)
\end{aligned}$$

577 and the average probability that radiation transferring from between-row background

578 to lateral “wall” is

$$\begin{aligned}
k_{C \rightarrow A(B)} &= \frac{1}{A_2} \int_0^{A_2} P_{C \rightarrow A(B)} dx, \\
579 \quad P_{C \rightarrow A(B)} &= \begin{cases} \frac{2}{\pi} \arctan\left(\frac{h \sin \varphi_{or}}{A_2}\right) & (x = A_2) \wedge (x = 0) \\ \frac{\arctan\left(\frac{h}{x}\right) + \arctan\left(\frac{h \sin \varphi_{or}}{A_2 - x \sin \varphi_{or}}\right)}{\pi} & x \in (0, A_2) \end{cases} \quad (E-6)
\end{aligned}$$

580 Eqs. (E , 2-6) are elements of matrix of transfer probability between lateral “wall”,

581 between-row background and escape surface. Therefore, the matrix of transfer

582 probability is

$$\begin{aligned}
583 \quad \mathbf{k}(x, z, \Omega' \rightarrow \Omega) &= \begin{cases} \begin{bmatrix} k_{B \rightarrow B} & k_{B \rightarrow A} & k_{B \rightarrow C} & k_{B \rightarrow escape} \\ k_{A \rightarrow B} & k_{A \rightarrow A} & k_{A \rightarrow C} & k_{A \rightarrow escape} \\ k_{C \rightarrow B} & k_{C \rightarrow A} & k_{C \rightarrow C} & k_{C \rightarrow escape} \\ k_{escape \rightarrow B} & k_{escape \rightarrow A} & k_{escape \rightarrow C} & k_{escape \rightarrow escape} \end{bmatrix} & 0^\circ \leq \varphi_s < 180^\circ \\ \begin{bmatrix} k_{A \rightarrow A} & k_{A \rightarrow B} & k_{A \rightarrow C} & k_{A \rightarrow escape} \\ k_{B \rightarrow A} & k_{B \rightarrow B} & k_{B \rightarrow C} & k_{B \rightarrow escape} \\ k_{C \rightarrow A} & k_{C \rightarrow B} & k_{C \rightarrow C} & k_{C \rightarrow escape} \\ k_{escape \rightarrow A} & k_{escape \rightarrow B} & k_{escape \rightarrow C} & k_{escape \rightarrow escape} \end{bmatrix} & 180^\circ \leq \varphi_s < 360^\circ \end{cases} \quad (E-7) \\
&= \begin{bmatrix} 0 & k_{B(A) \rightarrow A(B)} & k_{B(A) \rightarrow C} & k_{B(A) \rightarrow} \\ k_{B(A) \rightarrow A(B)} & 0 & k_{B(A) \rightarrow C} & k_{B(A) \rightarrow} \\ k_{C \rightarrow A(B)} & k_{C \rightarrow A(B)} & 0 & k_{C \rightarrow} \\ 0 & 0 & 0 & 0 \end{bmatrix}
\end{aligned}$$

584 **E-2 Light attenuation coefficient**

585 Radiation transfer in this area is influenced by two mediums, i.e., vegetation in
 586 two lateral “walls” (A' and B') and soil of between-row (C'). For attenuation
 587 coefficient in two lateral “walls”, we continue to use the attenuation coefficient for
 588 horizontal diffuse flux (n'). For attenuation coefficient for soil of between-row (a_s),
 589 we derived backward by using the modified Hapke model [14]. According to (pers.
 590 comm. W. Verhoef, 2018), there is

591
$$a_s = 2 - \frac{4r_s (\cos \theta_s + \cos \theta_o)}{p(\delta) \cos \theta_s^2 \cos \theta_o^2} \left(1 - \frac{b}{4}\right) \quad (\text{E-8})$$

592 Here $p(\delta)$ is the scattering phase function of soil particle, which represents the
 593 second-order Legendre polynomial (an approximation of spherical function) [15],

594 and $p(\delta) = 1 + b \cos \delta + c \frac{3 \cos^2 \delta - 1}{2}$, and $\cos \delta = \cos \theta_s \cos \theta_o + \sin \theta_s \sin \theta_o \cos \varphi_{so}$.

595 Here b and c are the adjustment parameters for the second-order Legendre
 596 polynomial in the scattering phase function of soil particle, and they can be
 597 determined by [16]. According to Eq. (E-7), and then combined with the calculation

598 rules of hadamard product (i.e.,

599 $\mathbf{K}(x, z, \Omega' \rightarrow \Omega) = \mathbf{k}(x, z, \Omega' \rightarrow \Omega) * \mathbf{a}(x, z, \Omega' \rightarrow \Omega)$, $\mathbf{a}(x, z, \Omega' \rightarrow \Omega)$ is the

600 matrix of light attenuation coefficient

601
$$\mathbf{a}(x, z, \Omega' \rightarrow \Omega) = \begin{bmatrix} 0 & n' & a_s & 0 \\ n' & 0 & a_s & 0 \\ n' & n' & 0 & 0 \\ 0 & 0 & 0 & 0 \end{bmatrix} \quad (\text{E-9})$$

602 E-3 Solving equations

603 Converting Eq. (E-1) into an operator notation, there is

$$604 \quad f = \mathbf{K}f + f_0 \quad (\text{E-10})$$

605 in which

$$606 \quad \mathbf{K}(x, z, \Omega' \rightarrow \Omega) = \mathbf{k}(x, z, \Omega' \rightarrow \Omega) * \mathbf{a}(x, z, \Omega' \rightarrow \Omega)$$

$$= \begin{bmatrix} 0 & n'k_{B(A) \rightarrow A(B)} & a_s k_{B(A) \rightarrow C} & k_{B(A) \rightarrow} \\ n'k_{B(A) \rightarrow A(B)} & 0 & a_s k_{B(A) \rightarrow C} & k_{B(A) \rightarrow} \\ n'k_{C \rightarrow A(B)} & n'k_{C \rightarrow A(B)} & 0 & k_{C \rightarrow} \\ 0 & 0 & 0 & 0 \end{bmatrix} \quad (\text{E-11})$$

607 According to the Riemann series principle, for $|\mathbf{K}| < 1$, and we let $f_0 = \mathbf{J}$. Eq.

608 (E-11) becomes

$$609 \quad f = \mathbf{J} + \mathbf{K}\mathbf{J} + \mathbf{K}^2\mathbf{J} + \dots \approx \mathbf{J} + \mathbf{J}\mathbf{K}(\mathbf{I} - \mathbf{K})^{-1} \quad (\text{E-12})$$

610 Eq. (E-12) represents the collision of radiation in the between-row, which is

611 composed of single scattering and multiple scattering (i.e., up to n-scattering). The

612 between-row area includes two lateral “walls” (A' and B'), between-row

613 background (C') and escaping surface ($abcd$ in Fig. D-1). The DRF on the A' , B' ,

614 C' and escaping surface should be the DRF of the soil of between-row (R_s) and the

615 DRF of the two lateral walls (R_b and R_d) and 0, respectively.

$$616 \quad R_s = \frac{r_s E_s(0)}{E_s(0) + E_-(0)} \quad (\text{E-13})$$

617 Then, we let single scattering of between-row for A' , B' , C' and escaping surface

618 be

$$619 \quad \mathbf{R}_{b_r_1} = \mathbf{J} = \begin{cases} \begin{bmatrix} R_b & R_d & R_s & 0 \end{bmatrix} & 0^\circ \leq \varphi_s < 180^\circ \\ \begin{bmatrix} R_d & R_b & R_s & 0 \end{bmatrix} & 180^\circ \leq \varphi_s < 360^\circ \end{cases} \quad (\text{E-14})$$

620 and substitute these initial values into Eq. (C-12), there is

$$621 \quad \mathbf{R}_{b_r} = \mathbf{R}_{b_{r-1}} + \mathbf{R}_{b_{r-m}} = \mathbf{J} + \mathbf{JK}(\mathbf{I} - \mathbf{K})^{-1} \quad (\text{E-15})$$

622 Here $\mathbf{R}_{b_{r-m}}$ is multiple scattering matrices of A' , B' , C' and escaping surface.

623 The final calculation result of $\mathbf{R}_{b_{r-m}}$ is $[R_{b_m} \ R_{d_m} \ R_{s_m} \ 0]^T$. In the

624 between-row, we focus on between-row background, i.e., multiple scattering of soil in

625 the between row, and both initial values are calculated to be the same value, there is

$$626 \quad R_{s_m} = \frac{a_s k_{B(A) \rightarrow C} (R_b + R_d) + 2a_s n' k_{B(A) \rightarrow C} k_{C \rightarrow A(B)} R_s}{1 - k_{B(A) \rightarrow A(B)} - 2a_s n' k_{B(A) \rightarrow C} k_{C \rightarrow A(B)}} \quad (\text{E-16})$$

627 References

- 628 1. W. Verhoef, "Theory of radiative transfer models applied in optical remote sensing of
629 vegetation canopies," Ph.D, Landbouw Universiteit Wageningen, Wageningen, 1998.
- 630 2. W. Verhoef, "Light scattering by leaf layers with application to canopy reflectance modeling:
631 The SAIL model," *Remote Sensing of Environment*, vol. 16, pp. 125-141, 1984.
- 632 3. Q. Chen, D. zhang, and G. wei, *Basics of real function and functional analysis*. BeiJing: Higher
633 Education Press, 1983.
- 634 4. A. Kuusk, "The hot-spot effect of a uniform vegetative cover," in *Sov. J. Remote Sensing*,
635 1985.
- 636 5. F. Zhao, X. Gu, W. Verhoef, Q. Wang, T. Yu, Q. Liu, *et al.*, "A spectral directional reflectance
637 model of row crops," *Remote Sensing of Environment*, vol. 114, pp. 265-285, 2010.
- 638 6. J. M. Chen and J. Cihlar, "Quantifying the effect of canopy architecture on optical
639 measurements of leaf area index using two gap size analysis methods," *Geoscience & Remote
640 Sensing IEEE Transactions on*, vol. 33, pp. 777-787, 1995.
- 641 7. J. M. Chen and T. A. Black, "Foliage area and architecture of plant canopies from sunfleck
642 size distributions," *Agricultural & Forest Meteorology*, vol. 60, pp. 249-266, 1992.
- 643 8. H. Gijzen and J. Goudriaan, "A flexible and explanatory model of light distribution and
644 photosynthesis in row crops," *Agricultural & Forest Meteorology*, vol. 48, pp. 1-20, 1989.
- 645 9. W. Qin and D. L. B. Jupp, "An analytical and computationally efficient reflectance model for
646 leaf canopies," *Agricultural & Forest Meteorology*, vol. 66, pp. 31-64, 1993.
- 647 10. W. Qin and N. S. Goel, "An evaluation of hotspot models for vegetation canopies," *Remote
648 Sensing Reviews*, vol. 13, pp. 121-159, 1995.
- 649 11. W. Verhoef, "Earth observation modeling based on layer scattering matrices," *Remote Sensing
650 of Environment*, vol. 17, pp. 165-178, 1985.
- 651 12. K. Liang, *Mathematical and physical methods*. BeiJing: Higher Education Press, 2010.

- 652 13. V. S. Antyufeev and A. L. Marshak, "Inversion of Monte Carlo model for estimating
653 vegetation canopy parameters," *Remote Sensing of Environment*, vol. 33, pp. 201-209, 1990.
- 654 14. W. Verhoef and H. Bach, "Coupled soil-leaf-canopy and atmosphere radiative transfer
655 modeling to simulate hyperspectral multi-angular surface reflectance and TOA radiance data,"
656 *Remote Sensing of Environment*, vol. 109, pp. 166-182, 2007.
- 657 15. B. Hapke, "Hapke, B.W.: Bidirectional reflectance spectroscopy 1: theory. J. Geophys. Res. 86,
658 3039-3054," *Journal of Geophysical Research Atmospheres*, vol. 221, 1981.
- 659 16. S. Jacquemoud, F. Baret, and J. F. Hanocq, "Modeling spectral and bidirectional soil
660 reflectance," *Remote Sensing of Environment*, vol. 41, pp. 123-132, 1992.
- 661